Supplementary Text

We designed gRNAs targeting *SOD1*, *TBK1*, and *TARDBP* for use with AsCpf1(S542R/K607R), a modified, highly efficient Cpf1 variant[1]. We first tested the efficacy of these guides in HEK293FT cells and selected the gRNA with the highest indel rate for each target (Supplementary Fig. 22). We next targeted these three genes in our engineered neural tissues using a dual vector system in which one vector contained hSyn1-promoter-driven AsCpf1(S542R/K607R) enabling specific targeting of human iN cells and the second vector contained the gRNA (Supplementary Fig. 23a,b). The second vector also included hSyn1-promoter-driven mCherry fluorescent protein, fused to KASH transmembrane domain, to enable fluorescent-activated cell sorting (FACS) of targeted human iN cells (Supplementary Fig. 23a). These vectors were packaged into adeno-associated viral vectors (AAVs), which were used to infect co-cultured iN cells in a 3D hydrogel matrix (Supplementary Fig. 23c).

Supplementary Methods

Immunostaining and imaging. For immunofluorescent staining of iN cells cultured on 2D for 2 weeks, cells on coverslips in 6-well plates were fixed with 4% paraformaldehyde for 20 min at room temperature (RT) and then washed 3 times with DPBS. Coverslips containing fixed cells were individually transferred to each well of a 24-well plate for immunostaining procedure. For immunofluorescent staining of iN cells 3D cultured in 200 μl 4.6 mg/ml Matrigel for 30 days without use of Ara-C, cell encapsulating hydrogels were fixed with 4% PFA for 1 h at RT and 2 h at 4 °C and then washed 3 times with DPBS at RT. These hydrogels were then frozen in freezing medium (Tissue-Tek O.C.T. Compound) and maintained at -80 °C overnight. Sections of cell encapsulating hydrogels were cut at 20 μm using a cryostat (Leica CM1950) and washed with DPBS to remove freezing medium before immonostaining. For immunofluorescent staining of astrocytic cells generated using "morphogen + fbs" condition, at day 35 cells were fixed on coverslips as previously described and transferred to the 24-well plate for immunostaining. Mouse astrocytes were fixed in the same manner for immunostaining. Samples were blocked with 5% normal goat serum (Sigma) and 0.15% Triton X-100 (Sigma) in DPBS for 1 h at RT. Samples were then incubated with primary antibodies in 2.5% normal goat serum and 0.1% Triton X-100 in DPBS overnight at 4 °C. Following the washing step 3 times with 0.1% Triton X-100 in DPBS, samples were incubated with secondary antibodies in 2.5% normal goat serum and 0.1% Triton X-100 in DPBS for 1 h at RT. After washing 3 times with 0.1% Triton X-100 in DPBS, samples were mounted using Prolong Diamond Antifade Mountant with DAPI (Thermo-Fisher Scientific) and imaged using a fluorescent microscope (Zeiss AX10). Quantification of astrocytic cells was performed using ImageJ software. Stem cells encapsulated in 200 μl 4.6 mg/ml Matrigel were stained with calcein (Thermo-Fisher Scientific) after 5 days of neural induction and imaged using a fluorescent microscope (Zeiss AX10). Day 2 phase images of iN cells encapsulated in Matrigel without Ara-C and phase images at different time points of cells exposed to astrocytic cell generation protocols were taken using the same microscope.

For immunofluorescent staining of iN cells 3D cultured in 200 µl 4.6 mg/ml Matrigel for 2 weeks with Ara-C, cell-laden hydrogels were fixed with 4% PFA for 1 h at RT and 2 h at 4 °C and then washed 3 times with DPBS at RT. Samples were immersed in blocking solution of 5% normal goat serum (Sigma) and 0.15% Triton X-100 (Sigma) in DPBS and placed on a shaker overnight at 4 °C. Samples were then immersed in a solution with a primary antibody in 2.5% normal goat serum and 0.1% Triton X-100 in DPBS and placed on a shaker for 24 h at 4 °C. Samples were washed 2 times with 0.1% Triton X-100 in DPBS and each wash was performed for 3 h on a shaker at RT. Samples were immersed in a solution with a secondary antibody in 2.5% normal goat serum and 0.1% Triton X-100 in DPBS and placed on a shaker for 18 h at RT. Samples were then washed as before. Immunostained cell-laden hydrogels were mounted using Prolong Diamond Antifade Mountant with DAPI on microscope slides by gently pressing them with coverslips and imaged using a confocal microscope (Zeiss LSM 710).

The following primary antibodies were used in this study: mouse anti-Map2 (M4403, Sigma, 1:300-500); rabbit anti-Pax6 (901301, BioLegend, 1:300); chicken anti-GFAP (ab4674, Abcam, 1:500); mouse anti-S100β (ab11178, Abcam, 1:500); rabbit anti-Vimentin (5741, Cell Signaling, 1:100). Secondary antibodies used in this study are: Alexa Fluor 488, 568 and/or 647 (Life Technologies, 1:500-1:1,000).

RT-qPCR. Total RNA isolates were used for quantitative PCR (qPCR) experiments. For qPCR validation experiments for 3D and 2D cultures of iN cells, 1 ng total RNA was used for each triplicate of each condition. For qPCR experiments of generation of astrocytic cells, 50 ng total RNA was used for each triplicate of each condition. For each sample, cDNA synthesis was carried out with RevertAid Reverse Transcription kit (Thermo-Fisher Scientific) using random hexamers and oligo-DT. RNA expression levels were quantified by qPCR using Taqman qPCR probes (Thermo-Fisher Scientific, Supplementary Table 16) and Fast Advanced Master Mix (Thermo-Fisher Scientific). qPCR was performed in 5 µl multiplexed reactions within 384-well plates using the LightCycler 480 Instrument II. Relative RNA expression was quantified by normalizing to GAPDH.

Electrophysiological measurements. Whole cell voltage-clamp and current-clamp recordings were performed for 3D cultures/co-cultures and 2D co-cultures of iN cells. 3D cultures/co-cultures and 2D co-cultures were infected with AAV U6-hSyn1-mCherry-KASH-hGH vectors encoding non-targeting sgRNA 6 days after forming the tissues to identify iN cells in 3D cultures during electrophysiological experiments. Recordings were performed in room temperature using K-Gluconate based intracellular solution (in mM: 131 K-Gluconate, 17.5 KCl, 9 NaCl, 10 HEPES, 1.1 EGTA, 1 $MgCl_2$, 2 Mg-ATP and 0.2 Na-GTP) and artificial cerebrospinal fluid (in mM: 119 NaCl, 2.3 KCl, 1 NaH_2PO_4, 11 Glucose, 26.2 $NaHCO_3$, 1.3 $MgCl_2$, 2.5 $CaCl_2$) as the external solution. Data were recorded using pClamp 10 (Molecular Devices). Spontaneous synaptic currents were recorded with the voltage clamped at -70 mV. Membrane capacitance and resistance were measured online using the built-in pClamp membrane test. The resting membrane potential was recorded under current clamp configuration.

Current voltage relationships of the neurons were also recorded under current clamp configuration, where changes in voltage and subsequent action potentials were recorded after injecting hyperpolarizing and depolarizing currents (-200 pA to +200 pA, 50 pA steps). All recordings were performed using a patch pipette with a resistance ranging from 3-5 mΩ.

Genome editing. Guides for Cpf1-mediated genome editing were analyzed for efficacy in human embryonic kidney 293FT (HEK293FT) cells. Each crRNA guide was cloned into a separate U6-driven crRNA expression plasmid (U6-crRNA-CMV-mCherry). An expression vector for the AsCpf1 S542R/K607R PAM variant (pcDNA3.1-CMV-AsCpf1(TYCV)-NLS-3xHA) was used as described previously[1]. HEK293FT cells were maintained in Dulbecco's modified Eagle's medium supplemented with 10% FBS (Gibco) at 37 °C with 5% CO_2 incubation. Cells were seeded one day prior to transfection in 96-well plates (Corning) at a density of approximately $2.4x10^4$ cells per well and transfected at 90-100% confluency using Lipofectamine 2000 (Invitrogen), according to the manufacturer's recommended protocol. A total of 100 ng Cpf1 plasmid and 50 ng crRNA expression plasmid were delivered per well. Cells were harvested using Quick Extract DNA extraction solution (Epicentre) according to the manufacturer's recommended protocol. Indel frequencies were quantified by deep sequencing as described previously[1].

For delivery, the AAV hSyn1-HA-NLS-AsCpf1(TYCV)-spA vector was generated by PCR amplifying the AsCpf1(TYCV) encoding sequence[1], and cloning of the resulting PCR template into AAV backbone[2] containing HA-NLS and a short poly A signal , under control of the human *Synapsin* 1 promoter (hSyn1). For the generation of AAV U6-hSyn1-mCherry-KASH-hGH vectors encoding sgRNAs targeting *SOD1, TBK1,* and *TARDBP* (plus a non-targeting control sgRNA), oligonucleotides (Integrated DNA Technologies) containing sgRNA sequences were annealed and cloned into AAV U6-DR(*Sap*I)-hSyn1-mCherry-KASH-hGH scaffold construct. All constructs were verified by Sanger sequencing.

High-titer AAV1/2 virions encoding AAV hSyn1-HA-NLS-AsCpf1(TYCV)-spA and AAV U6-hSyn1-mCherry-KASH-hGH vectors encoding sgRNAs targeting *SOD1, TBK1,* and *TARDBP* (plus a non-targeting control sgRNA) were produced as described previously[2]. Briefly, HEK293T cells were transfected with AAV1 and AAV2 serotype plasmids in equal ratios, transgene plasmid and pDF6 helper plasmid using polyethyleneimine. 72 h after transfection, cells were harvested and high-titer AAV1/2 virus was purified by iodixanol gradient ultracentrifugation as previously described[3,4]. The titer of AAV vectors was determined by real-time quantitative PCR (qPCR) using probe and primers specific for the hSyn1 promoter sequence (Integrated DNA Technologies).

Genome editing was performed in 3D human neural tissues formed by co-culturing 1:1 mixture of human iN cells and human astrocytic cells at a final cell concentration of $20x10^6$ cells/ml in 100 µl 3D hydrogels (7.36 mg/ml

Matrigel), and the culture mediums did not contain doxycycline, as described above. Astrocytic cells formed by following the protocol termed "morhogen + fbs" were cultured until day 70 (passage 3) and detached from culture plates with accutase for co-culturing with iN cells. 6 days after forming 3D human neural tissues, AAV infection was carried out using concentrated AAV constructs containing Cpf1 or targeting/non-targeting gRNAs. Each hydrogel encapsulated a total $2x10^6$ cells and was in 3 ml of neural culture medium. A 1:1 mixture of AAVs containing Cpf1 and AAVs containing targeting/non-targeting gRNA was mixed with 3 ml culture medium of each 3D tissue by having $40x10^3$ viral copies of each vector per cell. Each condition of targeting and non-targeting gRNA had two replicate tissues. After mixing AAV mixtures with culture mediums, 6-well plates containing 3D tissues were gently shaken for 1 min and then transferred to an incubator at 37 °C with 5% CO_2 atmosphere. For 5 days following AAV infection, the culture medium of 3D tissues was not changed. After that, one third of the whole culture medium was renewed with neural culture medium. 24 days after AAV infection, cells in 3D tissues were disassociated by following the protocol described above (see methods for 3D co-cultures of iN cells with human astrocytic cells and with human primary astrocytes). A population of $1x10^3$ $mCherry^+$ iN cells was collected by FACS for each disassociated 3D tissue in a well of 96-well plate containing 5 μl of QuickExtract DNA extraction buffer (Epicentre). The 96-well plate was then spun down at 2,000*g* for 1 min.

Cells suspended in QuickExtract DNA solution were incubated at 65 °C for 15 min, 68 °C for 15 min, and 98 °C for 10 min. Genomic DNA was PCR-amplified with Herculase II fusion polymerase over 28 cycles using locus-specific primers. An additional round of PCR was then performed to attach Illumina handles to amplicons for deep sequencing. Next-generation sequencing (NGS) was performed and indel frequencies were quantified as described previously[1]. For the targeting gRNA, one guide per locus was used. DNA from two biological replicates was used for NGS analysis. For the non-targeting control, DNA from two biological replicates was pooled for NGS analysis.

Supplementary Figures

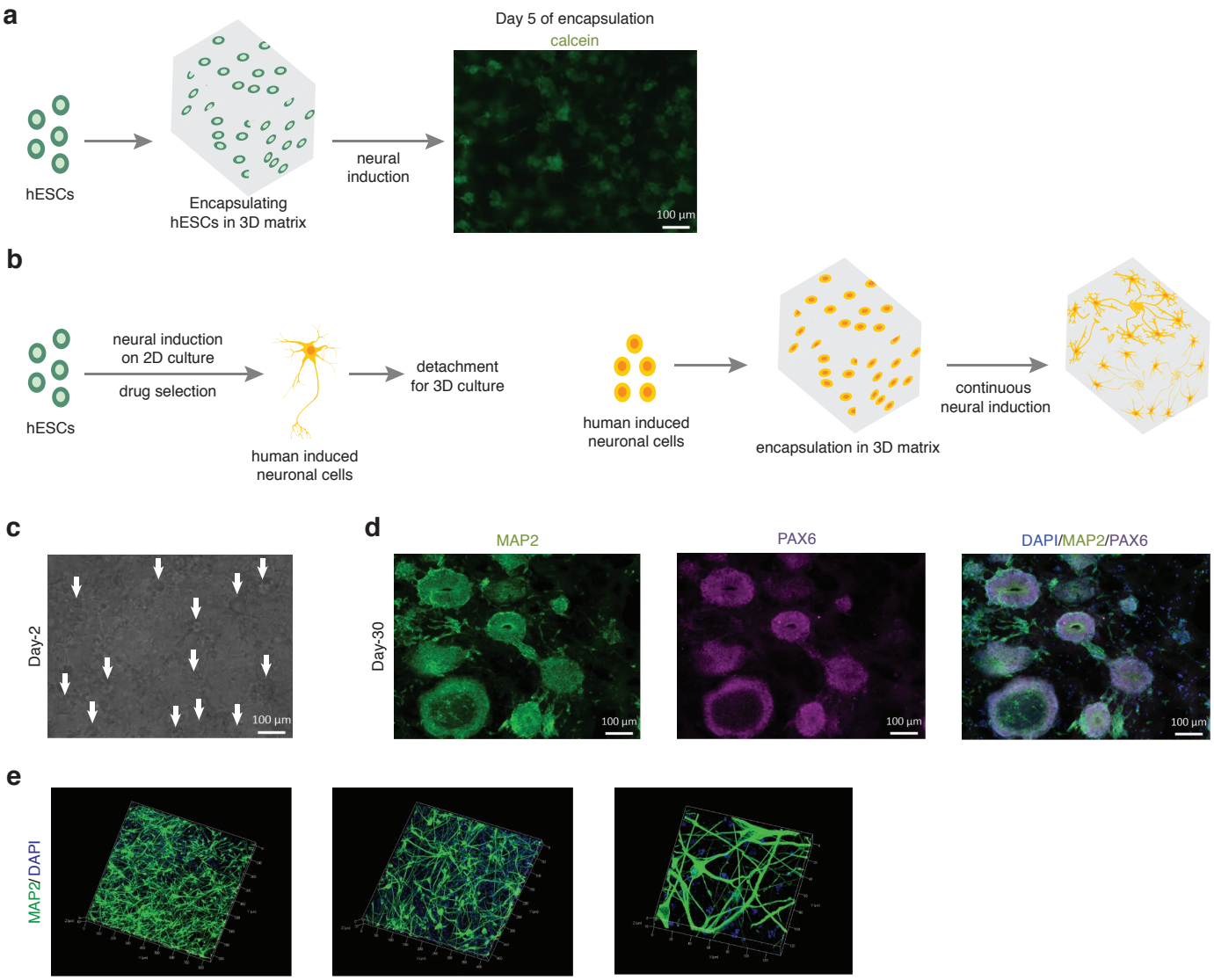

Supplementary Figure 1 | Method for generating pure 3D human neural tissue. (a) Schematic showing neural tissue formation by encapsulating hESCs within a 4.6 mg/ml Matrigel hydrogel and activating transcription factors (*NGN2* and *NGN1*) by delivering doxycyclin to cells in the matrix. Image of calcein stained 3D cultured cells at day 5 show encapsulated cells form aggregates. (b) Schematic showing neural tissue formation by first inducing neurons from hESCs on 2D cultures by activating transcription factors (*NGN2* and *NGN1*) followed by drug selection (puromycin), and then encapsulation of iN cells within a 4.6 mg/ml Matrigel hydrogel. (c) Phase image of encapsulated cells following neural induction on 2D cultures. Arrows point to cell aggregates formed in the hydrogel matrix within 2 days. (d) Cell aggregates formed in 3D (4.6 mg/ml) Matrigel hydrogels resulted in spheroids at day 30 which are shown by fluorescent images of cells stained with antibodies against MAP2 and PAX6. (e) Initial neural induction on 2D cultures was modified by performing stronger drug selection (puromycin) following transcription activation (*NGN2* and *NGN1*) in the presence of a proliferation inhibitor (Ara-C) introduced into culture medium after encapsulating cells in 3D (4.6 mg/ml Matrigel) matrix. Confocal z-stack images (with 10X, 20X, and 63X objectives) of pure 3D neural tissue at day 40 without cell aggregates formed by culturing iN cells in 4.6 mg/ml Matrigel (with MAP2 and DAPI staining).

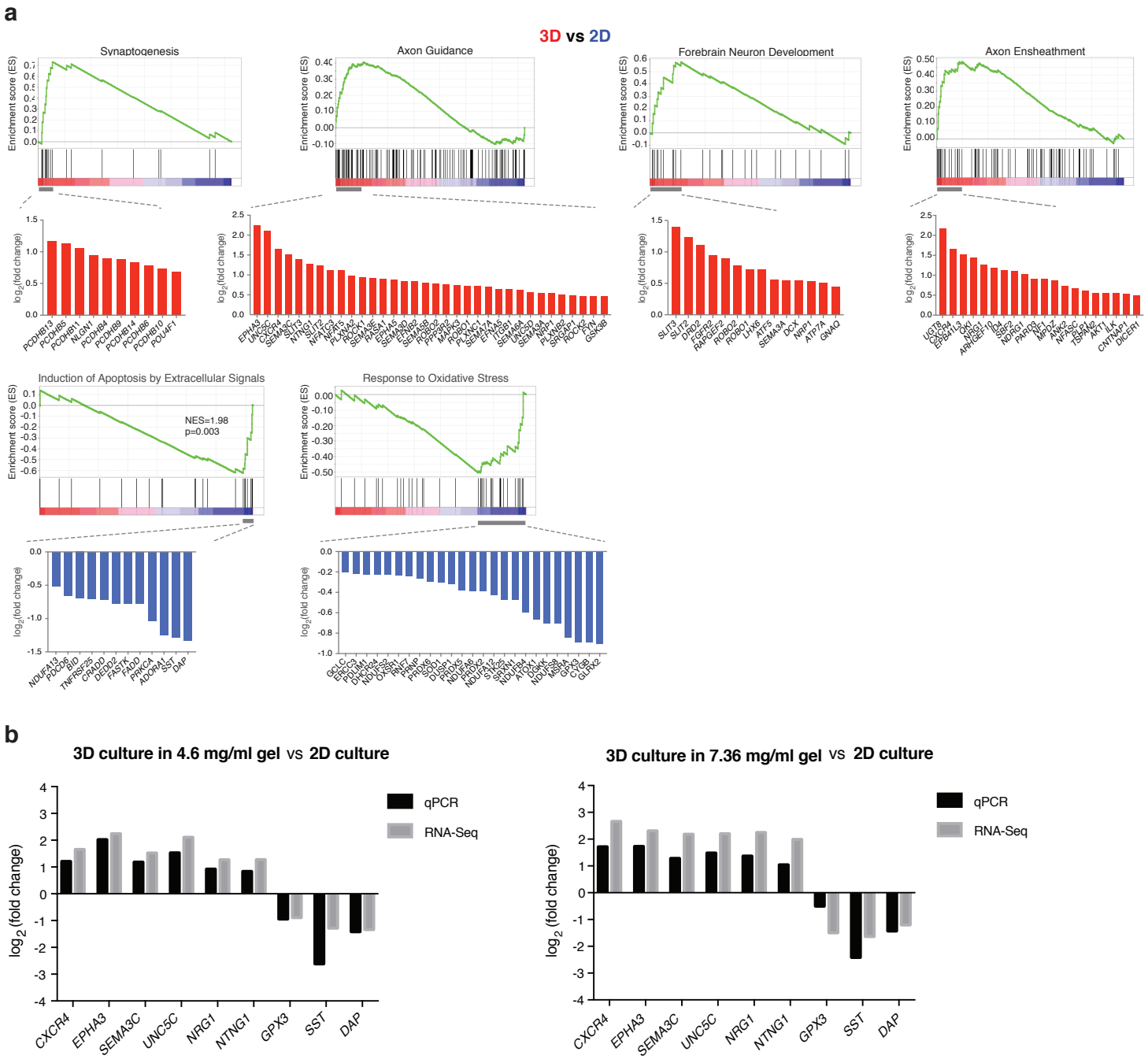

Supplementary Figure 2 | Analysis of 3D cultured iN cells. (a) Gene set enrichment analysis (GSEA) of representative enriched biological processes or signaling pathways in 3D (red) and 2D (blue) cultured iN cells at week 5 (represented in Fig. 1a,c). Normalized Enrichment Scores and nominal p values are shown as well as $\log_2$(fold change) (bottom) of genes contributing to core enrichment for each plot. (b) qPCR validation of selected genes from RNA-sequencing data at 5 weeks. (n=3 for all conditions).

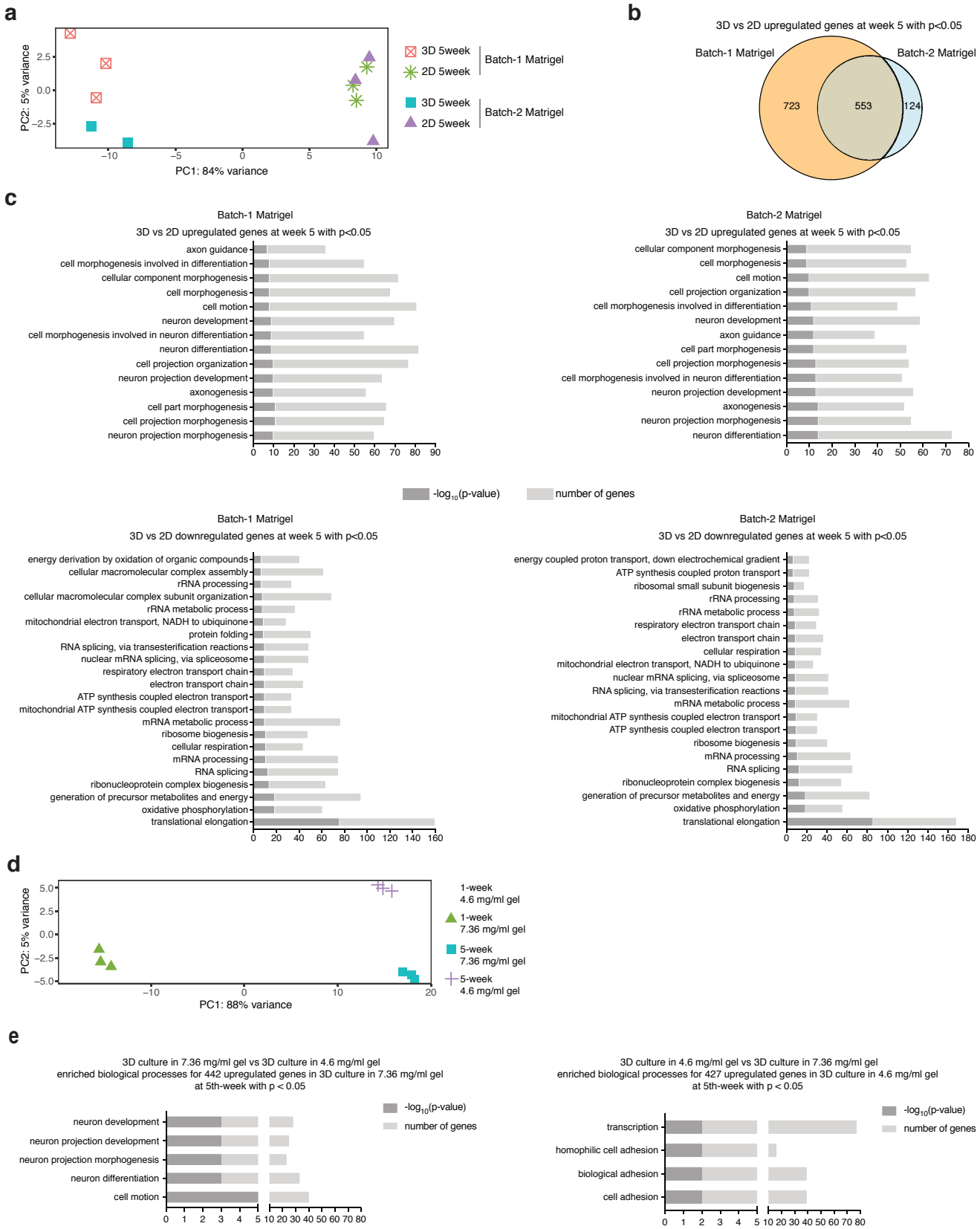

Supplementary Figure 3 | Analysis of the effect of batch and concentration of Matrigel on the gene expression profiles of 3D cultured iN cells. (a) Principal component analysis (PCA) of whole transcriptome data of 3D and 2D cultured iN cells at 1 week and 5 weeks (n=3 for each condition). For 3D cultures, human iN cells (at a concentration of $10x10^6$ cells/ml) were encapsulated in Matrigel (4.6 mg/ml) from two different batches, Batch-1 Matrigel and Batch-2 Matrigel. (b) Venn diagrams showing number of differentially upregulated genes with p<0.05 for 3D vs 2D cultures of iN cells

using two different batches of Matrigel and overlap genes at week 5 (adjusted p value is 0.05). (c) Gene ontology (GO) analysis for differentially upregulated and downregulated genes with $p<0.05$ for 3D vs 2D cultures of iN cells using two different batches of Matrigel (adjusted p value is 0.05). (d) PCA of whole transcriptome data of 3D cultured iN cells cultured (at $10x10^6$ cells/ml) in either 4.6 mg/ml or 7.36 mg/ml Matrigel (from same batch) at 1 week and 5 weeks (n=3 for each condition). (e) GO analysis for upregulated genes with $p<0.05$ in iN cells cultured within either 4.6 mg/ml or 7.36 mg/ml Matrigel at week 5. Differential expression analysis between 3D cultures in 4.6 mg/ml and 7.36 mg/ml Matrigel was performed by taking adjusted p value 0.05.

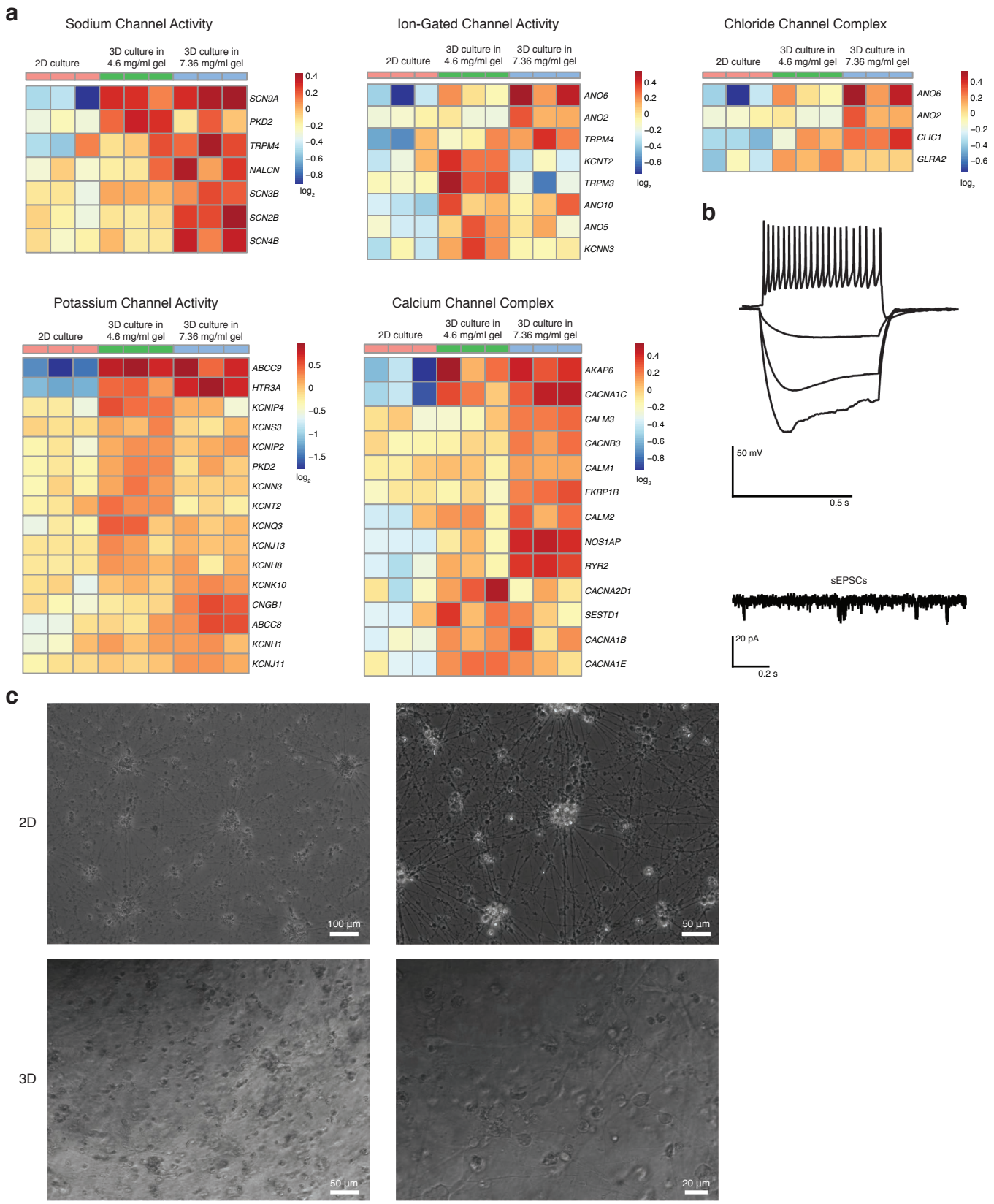

Supplementary Figure 4 | Long-term culture of iN cells in 3D hydrogels promotes expression of some genes associated with channels and healthy electrophysiological properties relative to iN cells on 2D cultures. (a) Relative expression of genes associated with channel activity and channel complexes showing significant ($p<0.05$) upregulation in iN cells cultured either within 4.6 mg/ml or 7.36 mg/ml Matrigel compared to 2D cultured iN cells at 5 weeks (n=3 for each condition). (b) iN cells cultured in 7.36 mg/ml Matrigel at 36 days exhibit neuronal excitability and spontaneous excitatory postsynaptic currents (sEPSCs) (n=6 iN cells). 3 out of 6 patched 3D cultured iN cells showed spontaneous activity. iN cells were patched while they were in the 3D matrix; 2D cultured iN cells at same time point could not be patched. (c) Representative phase images at week 5 of 2D cultured iN cells and 3D cultured iN cells (in 7.36 mg/ml Matrigel).

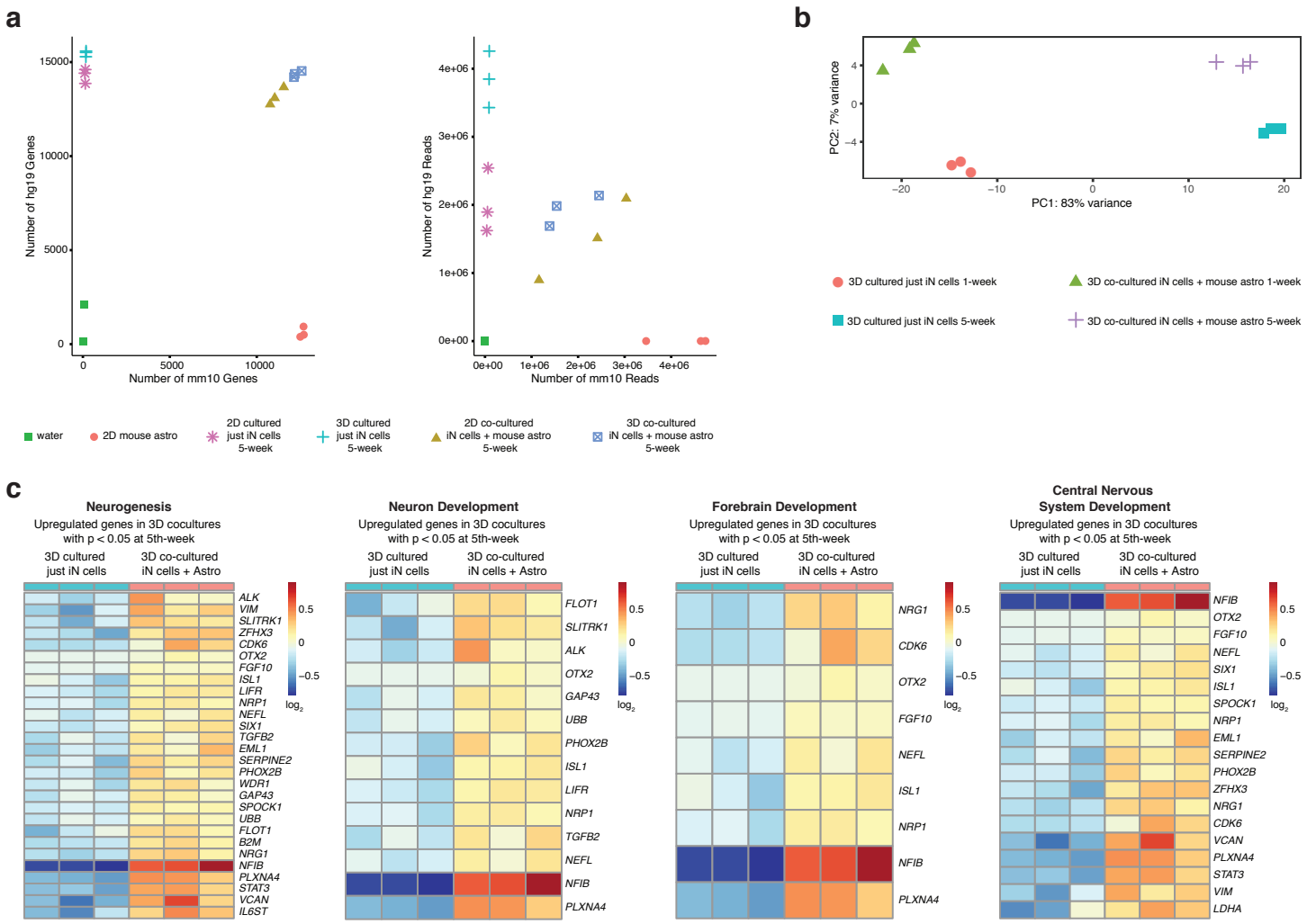

Supplementary Figure 5 | Filtering mouse reads from RNA-seq data involving co-cultures of human iN cells with mouse astrocytes and analysis of the effect of 3D co-culture of human iN cells with mouse astrocytes on gene expression profile of human iN cells. (a) We compare the number of mouse genes expressed to the number of human genes expressed in each sample, as well as comparing the number of reads mapping to mouse (excluding those mapping to Rn45s) to the number of reads mapping to human. Note these results are based on running RSEM using a joint human and mouse transcriptome. We see that samples consisting only of mouse cells have very little contaminating human reads and vice versa, while mixed samples contain both. (b) PCA for whole-transcriptome data of iN cells in 3D co-cultures (iN cells + mouse astro) or pure iN cells cultures (just iN cells) at 1 week and 5 weeks (n=3 for each condition). For co-cultures, iN cells derived from hESCs and mouse astrocytes (1:1 ratio at total $20x10^6$ cells/ml) were co-cultured in 3D (4.6 mg/ml Matrigel) hydrogels. For pure iN cells cultures, iN cells (at $10x10^6$ cells/ml) were cultured in 3D (4.6 mg/ml Matrigel) hydrogels. (c) Relative expression of genes significantly ($p<0.05$) upregulated in 3D co-cultured iN cells compared to 3D pure cultures of iN cells at 5 weeks associated with neurological processes.

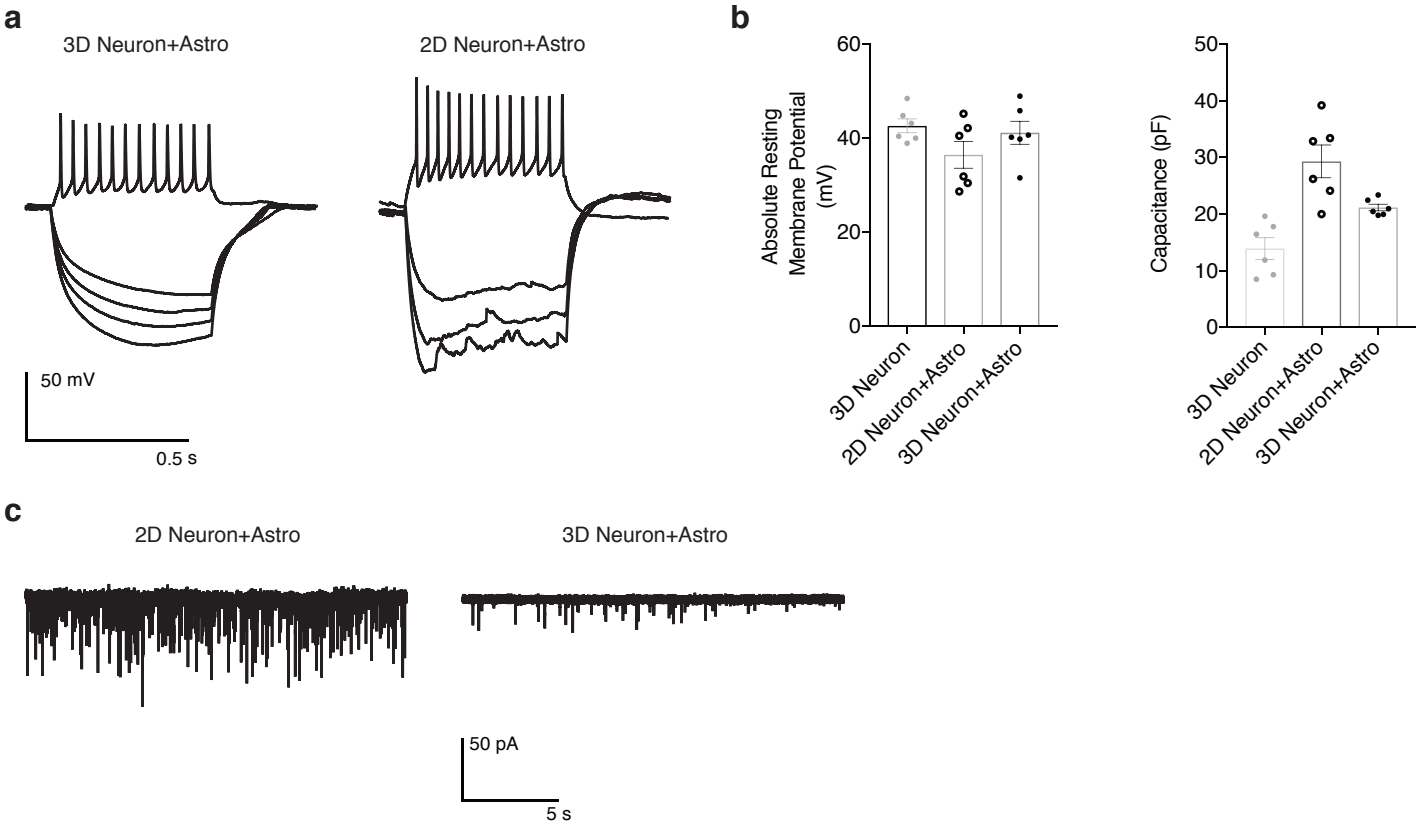

Supplementary Figure 6 | Electrophysiological properties of 3D cultured/co-cultured or 2D co-cultured iN cells. Human iN cells cultured with or without mouse astrocytes in 3D hydrogels (7.36 mg/ml Matrigel) and co-cultured with mouse astrocytes on 2D surfaces. Electrophysiological measurements on iN cell cultures with and without astrocytes in 3D hydrogels were conducted at day 45 and 36, respectively. Electrophysiological measurements on iN cell co-cultures on 2D surfaces were conducted at day 44. (a) Plots demonstrating excitability iN cells co-cultured with mouse astrocytes (Neuron+Astro) in a 3D hydrogel (7.36 mg/ml Matrigel) or on a 2D surface. (b) Absolute resting membrane potential and membrane capacitance for iN cells co-cultured with mouse astrocytes (Neuron+Astro) either in 3D or on 2D and 3D only iN cell cultures (Neuron) are shown. Each dot represents an absolute resting membrane potential value or a membrane capacitance value for a neuronal cell in a culture condition. Error bars show mean ± SEM. (c) Plots showing representative sEPSCs of human iN cells co-cultured with mouse astrocytes (Neuron+Astro) in 3D hydrogels (7.36 mg/ml Matrigel) (n=6 iN cells were measured for spontaneous activity) or on 2D surfaces (n=5 iN cells were measured for spontaneous activity). 6 out of 6 3D co-cultured iN cells showed spontaneous activity, while 5 out of 5 2D co-cultured iN cells showed spontaneous activity.

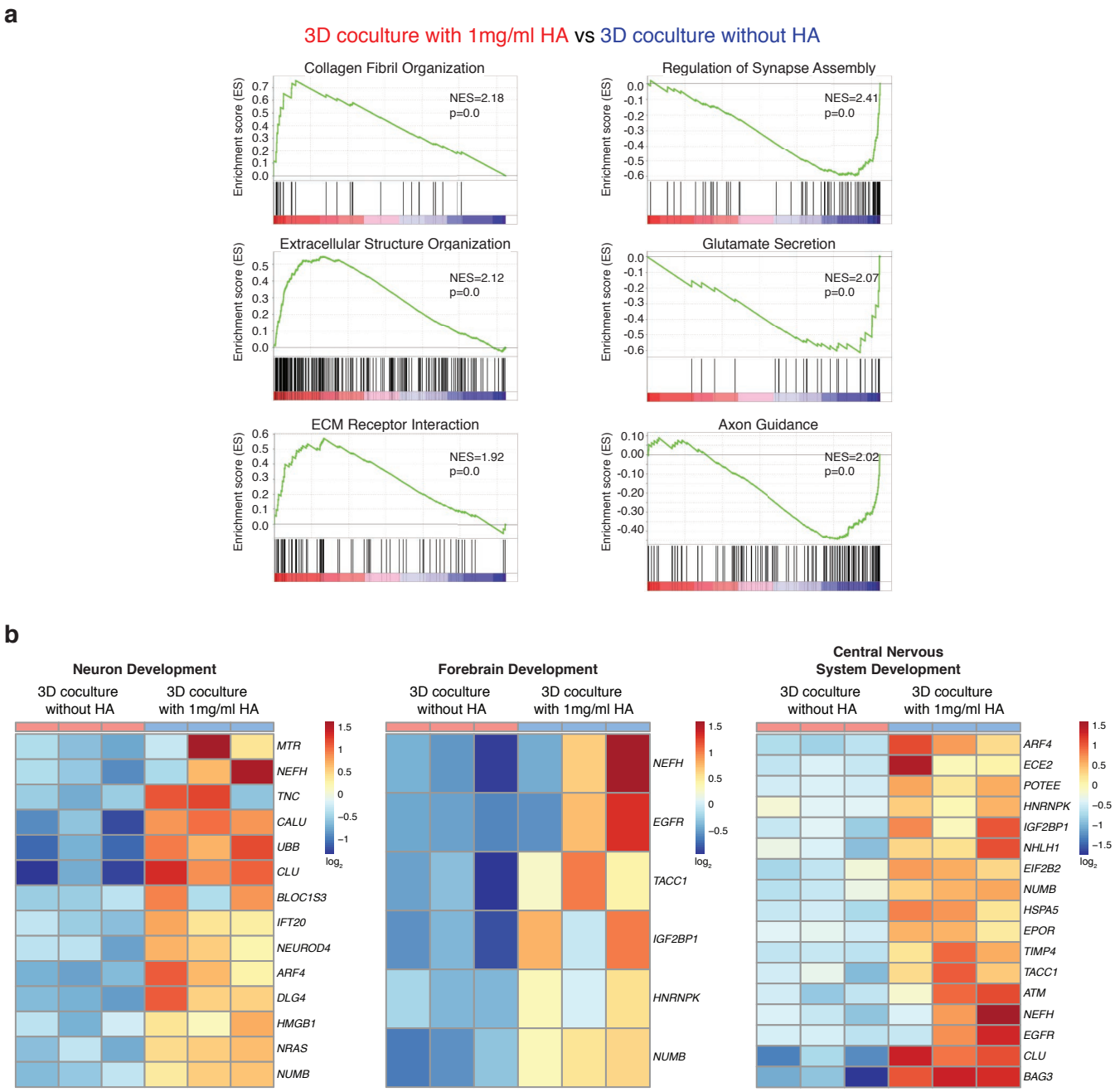

Supplementary Figure 7 | Analysis of gene expression profiles of human iN cells co-cultured in Matrigel with HA. (a) Human iN cells and mouse astrocytes (at a concentration of $30x10^6$ cells/ml) encapsulated in Matrigel with or without HA trapped within the Matrigel. GSEA of enriched non-neuronal biological processes and signaling pathways in iN cells co-cultured in Matrigel doped with HA relative to without HA. (b) Relative expression of significantly ($p < 0.05$) upregulated genes in iN cells co-cultured in 3D (7.36 mg/ml) Matrigel with HA compared to iN cells co-cultured in 3D (7.36 mg/ml) Matrigel without HA associated with neuron development, forebrain development and central nervous

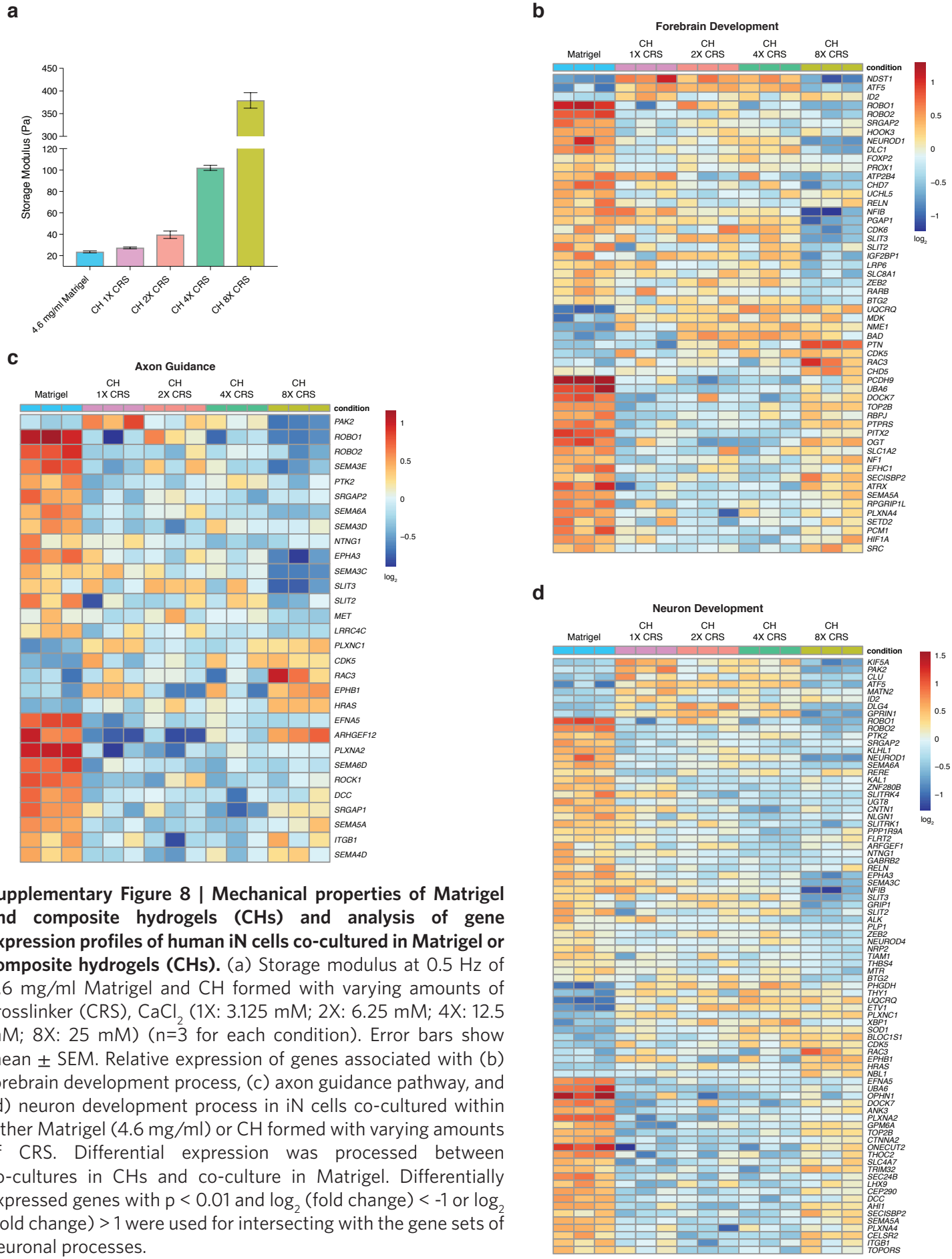

Supplementary Figure 8 | Mechanical properties of Matrigel and composite hydrogels (CHs) and analysis of gene expression profiles of human iN cells co-cultured in Matrigel or composite hydrogels (CHs). (a) Storage modulus at 0.5 Hz of 4.6 mg/ml Matrigel and CH formed with varying amounts of crosslinker (CRS), $CaCl_2$ (1X: 3.125 mM; 2X: 6.25 mM; 4X: 12.5 mM; 8X: 25 mM) (n=3 for each condition). Error bars show mean ± SEM. Relative expression of genes associated with (b) forebrain development process, (c) axon guidance pathway, and (d) neuron development process in iN cells co-cultured within either Matrigel (4.6 mg/ml) or CH formed with varying amounts of CRS. Differential expression was processed between co-cultures in CHs and co-culture in Matrigel. Differentially expressed genes with $p < 0.01$ and $\log_2$ (fold change) < -1 or $\log_2$ (fold change) > 1 were used for intersecting with the gene sets of neuronal processes.

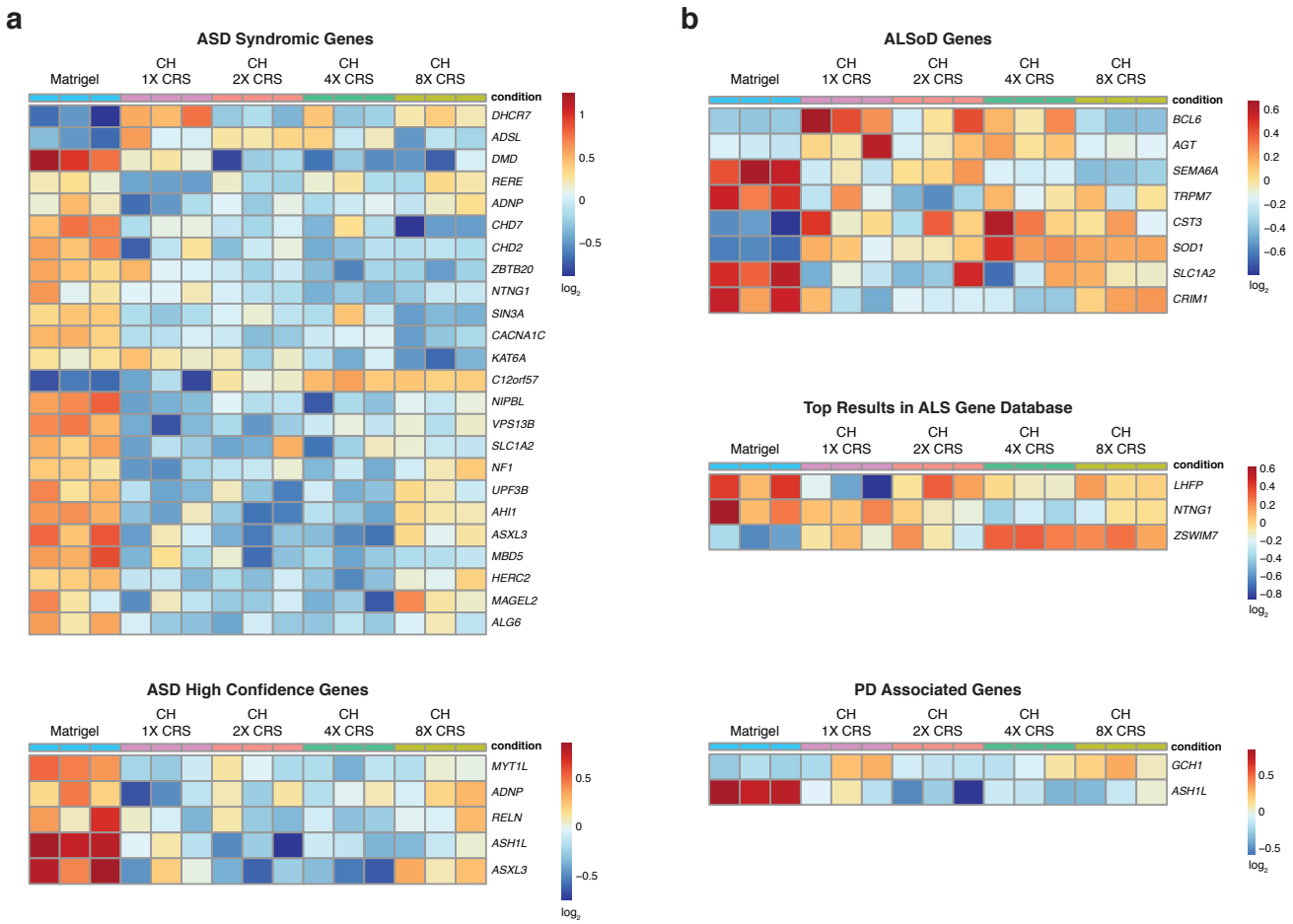

Supplementary Figure 9 | Expression profiles of disease-associated genes in iN cells co-cultured in Matrigel or composite hydrogels (CHs). Relative expression levels of (a) Autism Spectrum Disorder (ASD)-associated syndromic genes (from https://gene.sfari.org/autdb/GSGeneList.do?c=S) and ASD-associated high confidence genes (https://gene.sfari.org/autdb/GSGeneList.do?c=1), (b) Amyotrophic Lateral Sclerosis (ALS)-associated genes from ALS Online Database (ALSoD)[5] (http://alsod.iop.kcl.ac.uk/misc/dataDownload.aspx#C1), ALS-associated genes which are top results in ALS Gene Database[6] (http://www.alsgene.org/top_results) and Parkinson's Disease-associated genes[7] (http://www.pdgene.org/top_results) in iN cells co-cultured within either Matrigel (4.6 mg/ml) or CH formed with varying amounts of crosslinker (CRS), $CaCl_2$ (1X: 3.125 mM; 2X: 6.25 mM; 4X: 12.5 mM; 8X: 25 mM) (n=3 for each condition). Differential expression was processed between co-cultures in CHs and co-culture in Matrigel. Differentially expressed genes with $p < 0.01$ and $\log_2$ (fold change) < -1 or $\log_2$ (fold change) > 1 were used for intersecting with the disease-associated gene sets.

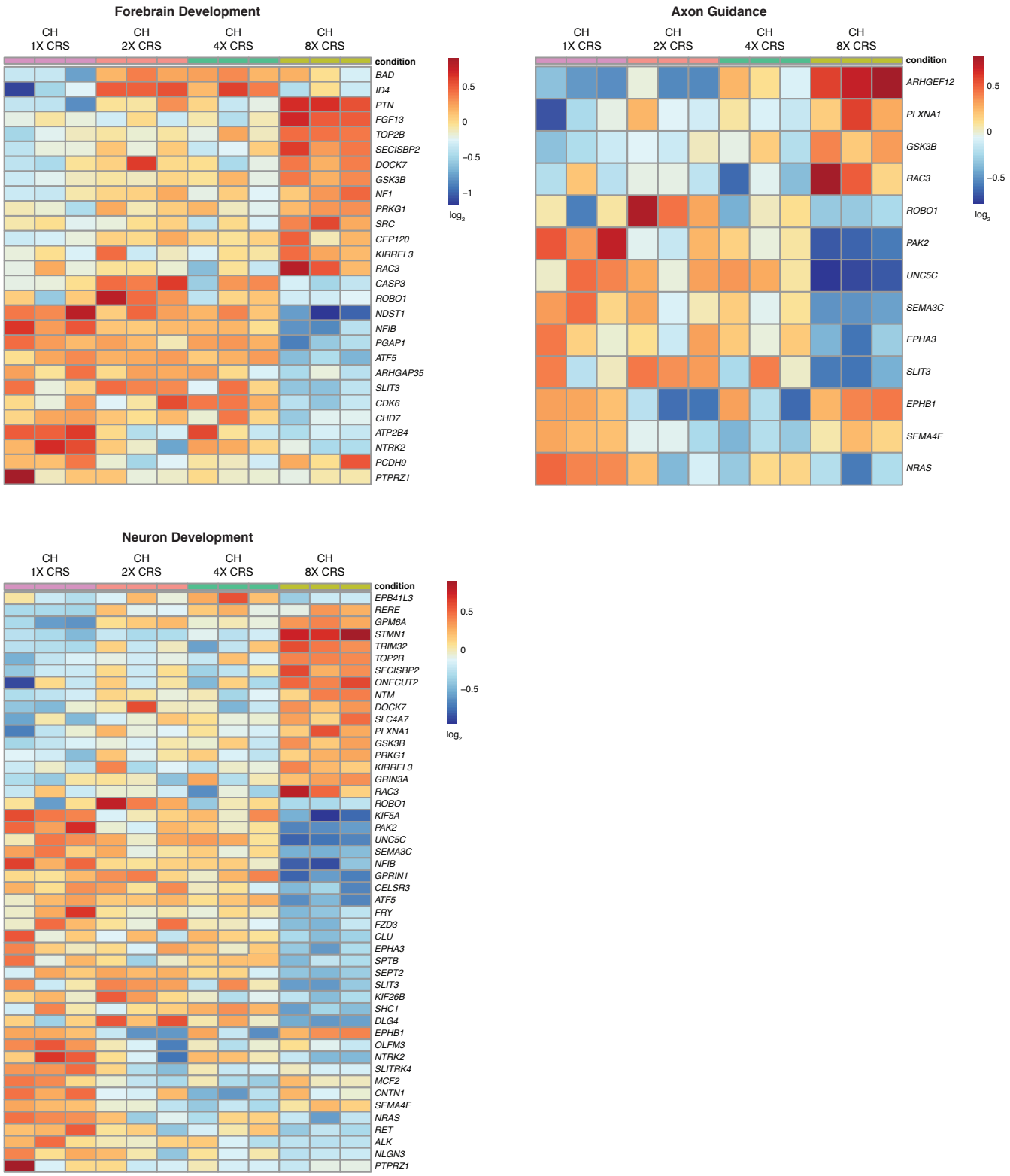

Supplementary Figure 10 | Analysis of the effect of varying amounts of CRS in CHs on expression of genes involved in neuronal processes. Relative expression of genes involved in forebrain development process, axon guidance pathway and neuron development process in iN cells co-cultured within CHs formed with varying amounts of $CaCl_2$ (1X: 3.125 mM; 2X: 6.25 mM; 4X: 12.5 mM; 8X: 25 mM). Differential expression analysis was performed as described in Fig. 4a and differentially expressed genes with $p < 0.05$ and $\log_2$ (fold change) < -0.75 or $\log_2$ (fold change) > 0.75 were further used for intersecting with the gene sets of neuronal processes.

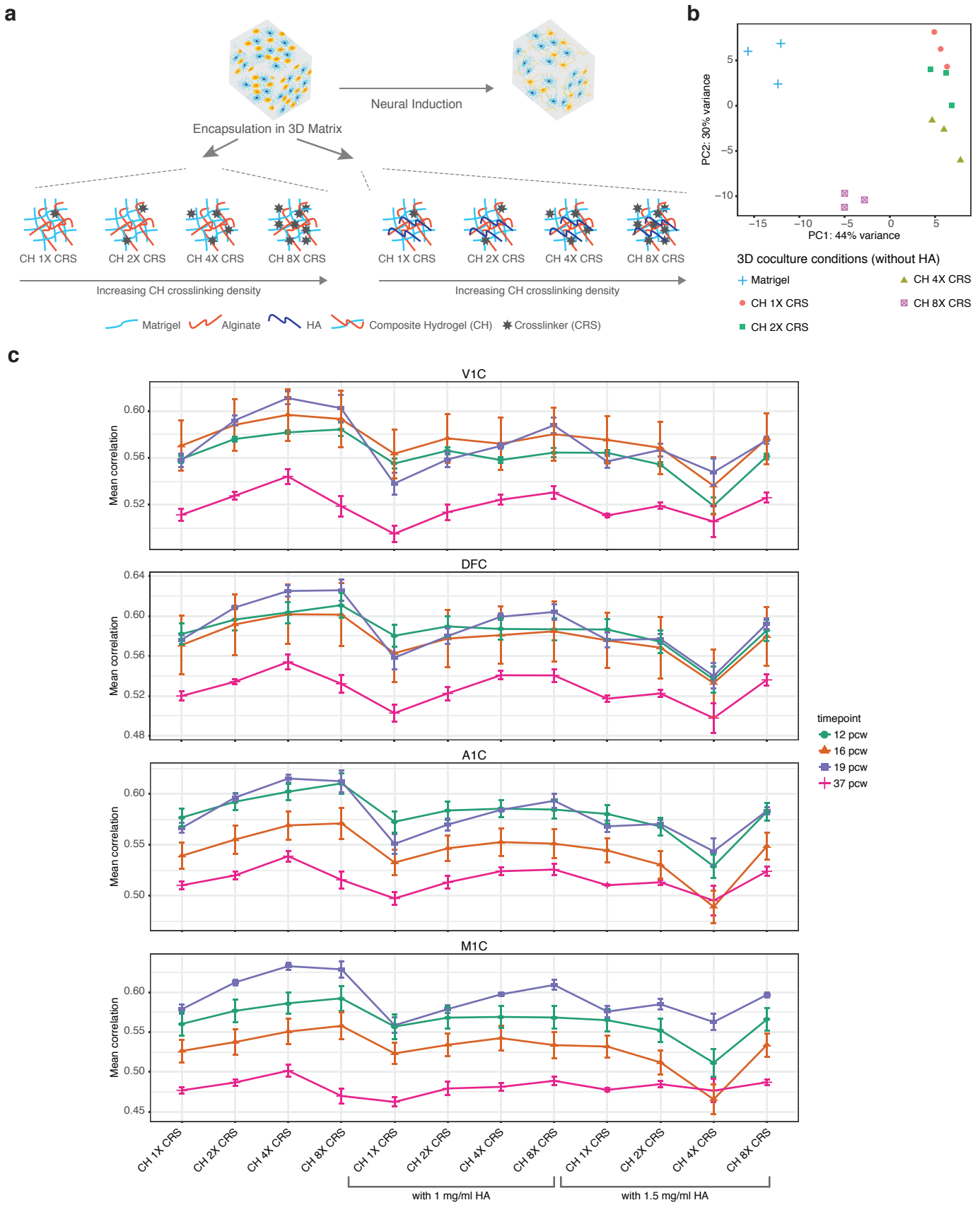

Supplementary Figure 11 | Analysis of the effect of HA on the transcriptome of 3D co-cultured human iN cells in CHs with varying amounts of CRS. (a) Schematic showing generation of 3D co-cultures of human iN cells and mouse astrocytes (at a concentration of $30x10^6$ cells/ml) to evaluate the addition of HA (either at 1 mg/ml or at 1.5 mg/ml concentration) within a CH of Matrigel (4.6 mg/ml) and alginate (5 mg/ml) with varying amounts of $CaCl_2$ (1X: 3.125 mM; 2X: 6.25 mM; 4X: 12.5 mM; 8X: 25 mM). (b) PCA based on whole-transcriptome data of co-cultured iN cells in

CHs without HA at week 5 (n=3 for each condition). (c) Pearson's correlation analysis comparing RNA-sequencing data of co-cultured human iN cells in CH with/without two different concentrations of HA with varying amounts of CRS to human brain transcriptome data of 4 different subregions at 4 fetal developmental stages. V1C: primary visual cortex (striate cortex, area V1/17); DFC: dorsolateral prefrontal cortex; A1C: primary auditory cortex (core); M1C: primary motor cortex (area M1, area 4). pcw: post-conceptual weeks. Bars show mean correlation ± SEM.

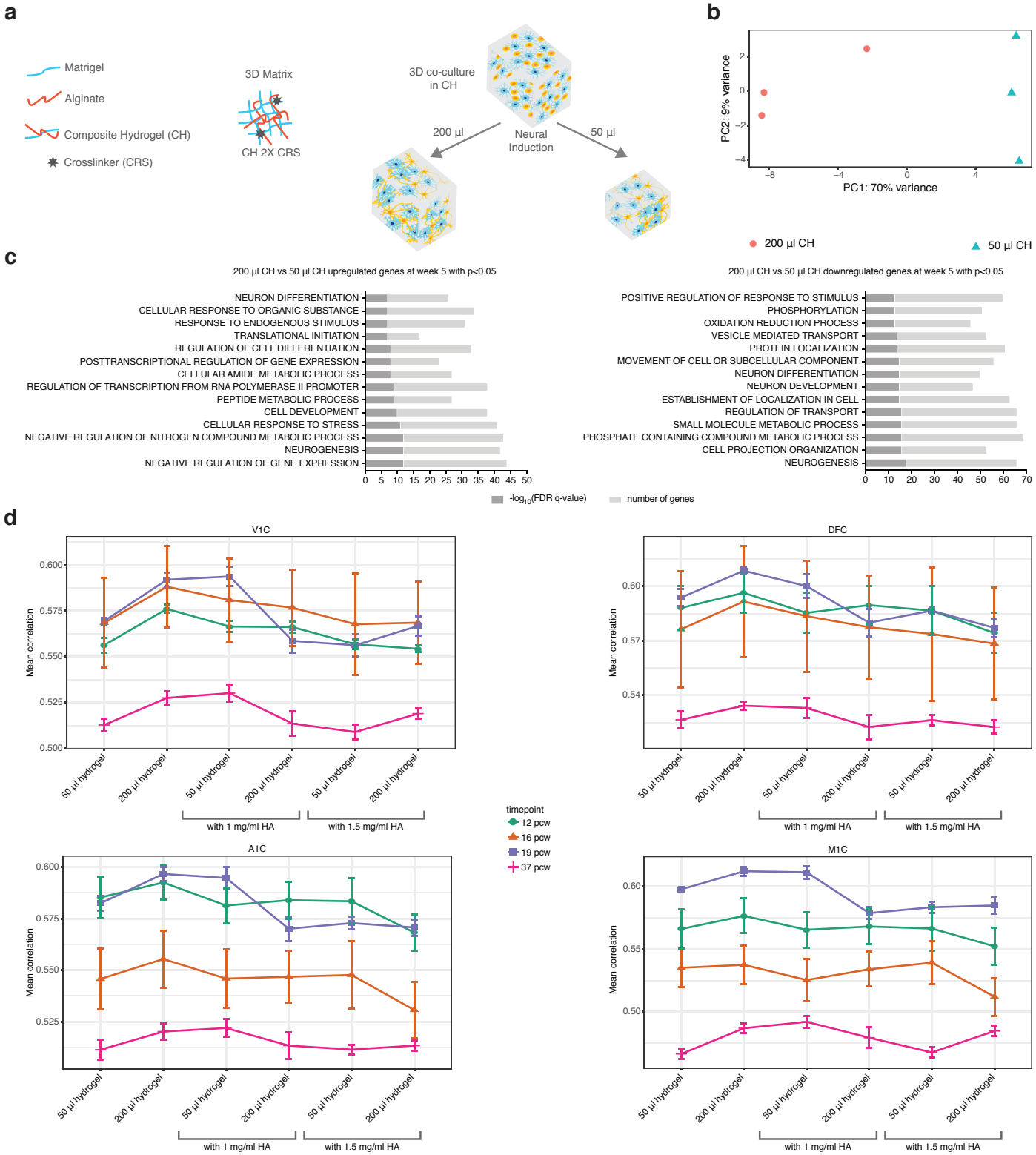

Supplementary Figure 12 | Influence of varying the volume of CH on gene expression in 3D co-cultured human iN cells. (a) Schematic showing generation of 3D co-cultures of human iN cells and mouse astrocytes (with 30x10^6 cells/ml) in either 200 µl or 50 µl CH (4.6 mg/ml Matrigel and 5 mg/ml alginate) with 2X CRS (6.25 mM $CaCl_2$). (b) PCA based on whole-transcriptome data of co-cultured iN cells at week 5 in two different volumes of CHs (n=3 for each condition). (c) GO analysis for differentially upregulated and downregulated genes with p<0.05 for co-culture of iN cells in 200 µl CH vs co-culture of iN cells in 50 µl CH (adjusted p value is 0.05). FDR: False Discovery Rate. (d) Pearson's correlation analysis of RNA-sequencing data of co-cultured human iN cells in two different volumes of CHs (with 2X CRS) with or without two different concentrations of HA compared to human brain transcriptome data of 4 different subregions at 4 fetal developmental stages. V1C: primary visual cortex (striate cortex, area V1/17); DFC: dorsolateral prefrontal cortex; A1C: primary auditory cortex (core); M1C: primary motor cortex (area M1, area 4). pcw: post-conceptual weeks. Bars show mean correlation ± SEM. (n=3 for each 3D culture condition, except n=2 for 50 µl CH with 1.5 mg/ml HA).

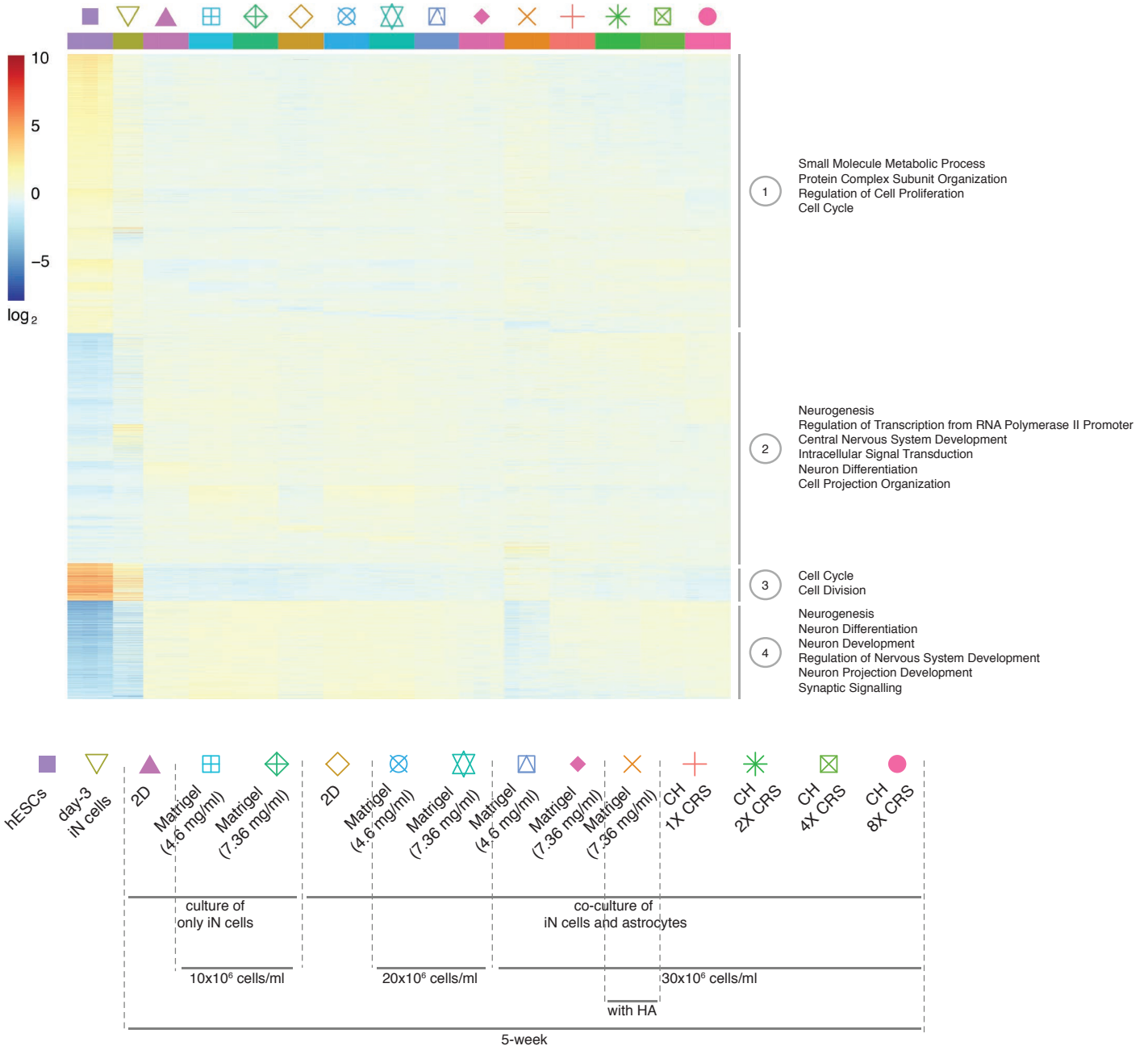

Supplementary Figure 13 | Gene expression clusters of iN cells cultured/co-cultured in different culturing conditions relative to hESCs. Differential expression was performed for each condition relative to hESCs (n=3 for each condition, except n=2 for condition of day 3 iN cells) (symbols are shown at the bottom of the figure). Differentially expressed genes for each condition relative to hESCs with $p < 0.01$ and $\log_2$ (fold change) < -2 or $\log_2$ (fold change) > 2 were used. Differentially expressed genes for all conditions were then combined. Heatmap displays the relative expression of combined genes as 4 clusters in iN cells cultured or co-cultured with mouse astrocytes in various conditions and in hESCs. Representative enriched GO terms for genes in each cluster are shown.

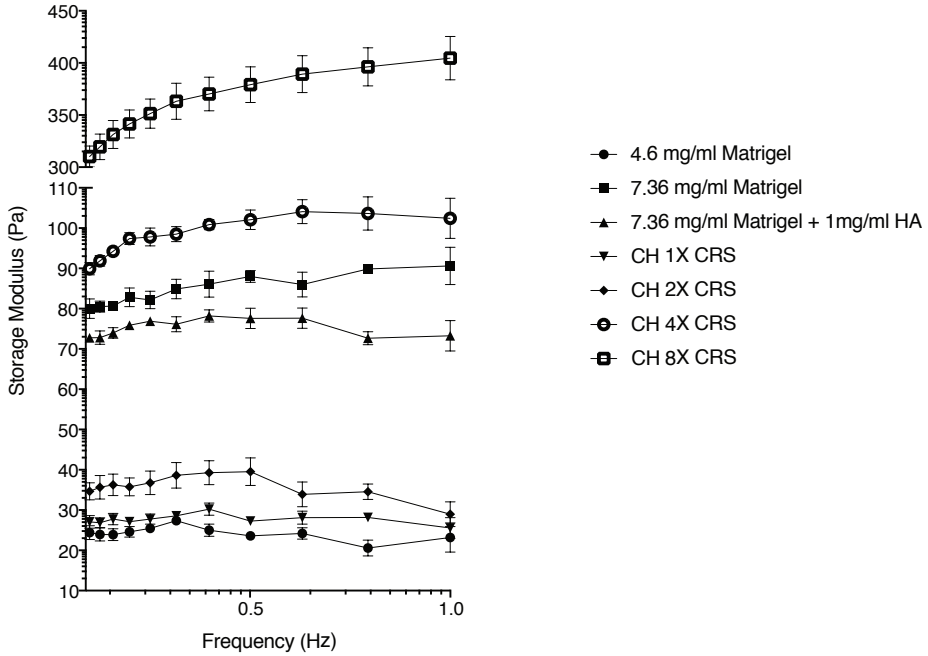

Supplementary Figure 14 | Frequency dependent rheology of various encapsulating hydrogels. Frequency dependent rheology of Matrigel at two different concentrations, Matrigel with HA, and CHs with varying amounts of CRS, $CaCl_2$ (1X: 3.125 mM; 2X: 6.25 mM; 4X: 12.5 mM; 8X: 25 mM) (n=3 for each condition). Bars show mean ± SEM.

Supplementary Figure 15 | Global comparison of effects of culture conditions on human iN cells. (a) Pearson's correlations between RNA-sequencing data of human iN cells cultured/co-cultured in different 3D conditions at 5 weeks (n=3 for each condition) (symbols are shown at the bottom of the figure) and human brain transcriptome data of 2 different subregions at 3 fetal developmental stages. A1C: primary auditory cortex (core); M1C: primary motor cortex (area M1, area 4); pcw: post-conceptual weeks. Each dot shows a correlation value between a 3D condition and a brainspan sample. Each brainspan timepoint-region pair has 1 sample except for 12 pcw, which had 3 samples available for each subregion. Bars show mean correlation ± SEM. (b) Expression levels of selected disease-associated genes across various 3D conditions encapsulating human iN cells (ASD, autism spectrum disorder; ALS, amyotrophic lateral sclerosis; AD, Alzheimer's disease; PD, Parkinson's disease). Color schemes are based on z-score distribution.

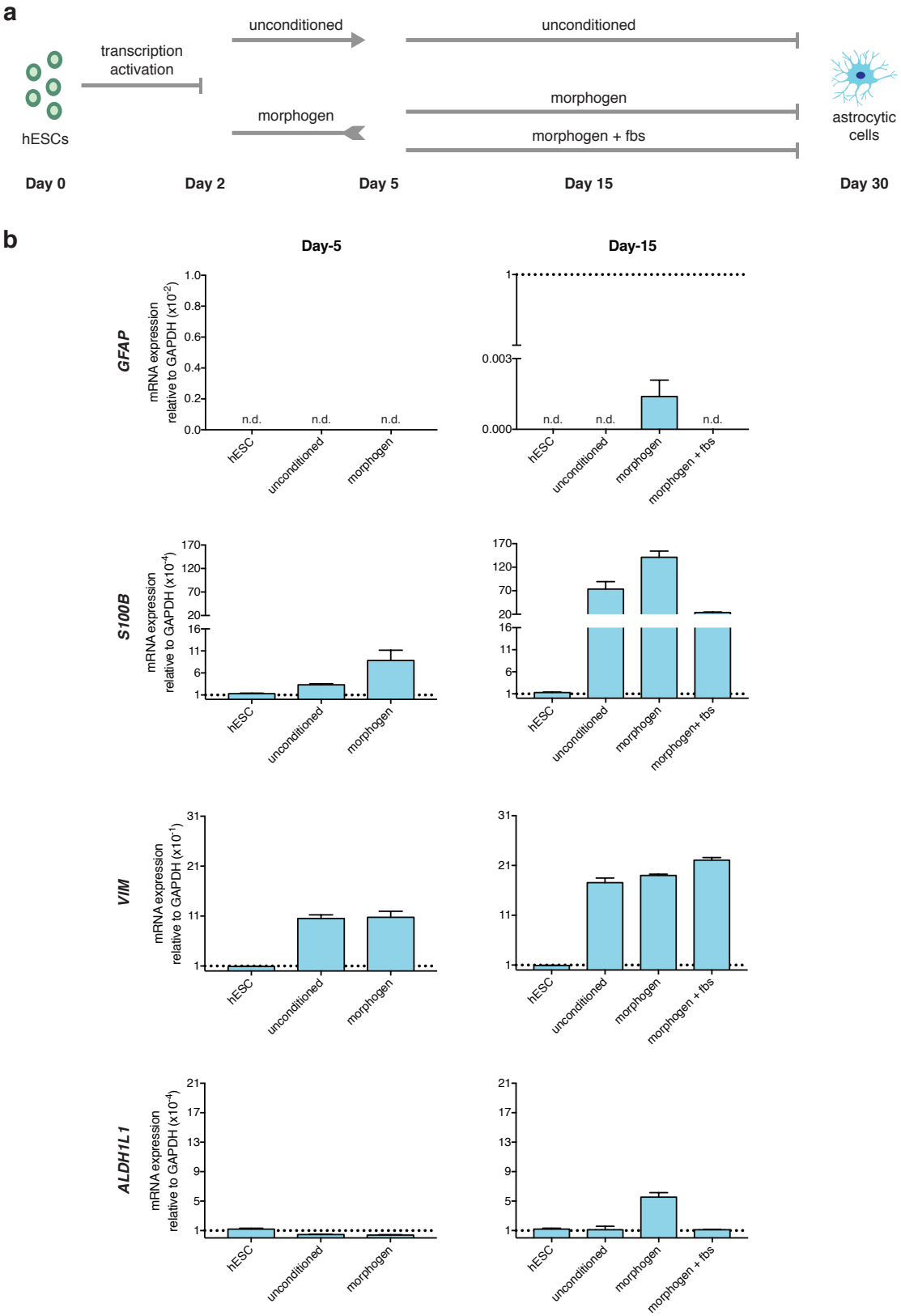

Supplementary Figure 16 | Derivation of human astrocytic cells directly derived from hESCs. (a) Schematic showing generation of human astrocytic cells from hESCs by combining transcription factors (*NGN1* and *NGN2*) used for neural induction, a morphogen (cntf, ciliary neurotrophic factor) and fetal bovine serum (fbs). (b) Expression of *GFAP*, *S100B*, *VIM* and *ALDH1L1* in treated cells at day 5 and day 15. Undifferentiated hESCs were used as negative control. (Expression levels for human primary astrocytes used as positive control can be found in Supplementary Fig. 18b). (n=3 for all conditions and bars show mean ± SEM). (n.d. represents not-detected).

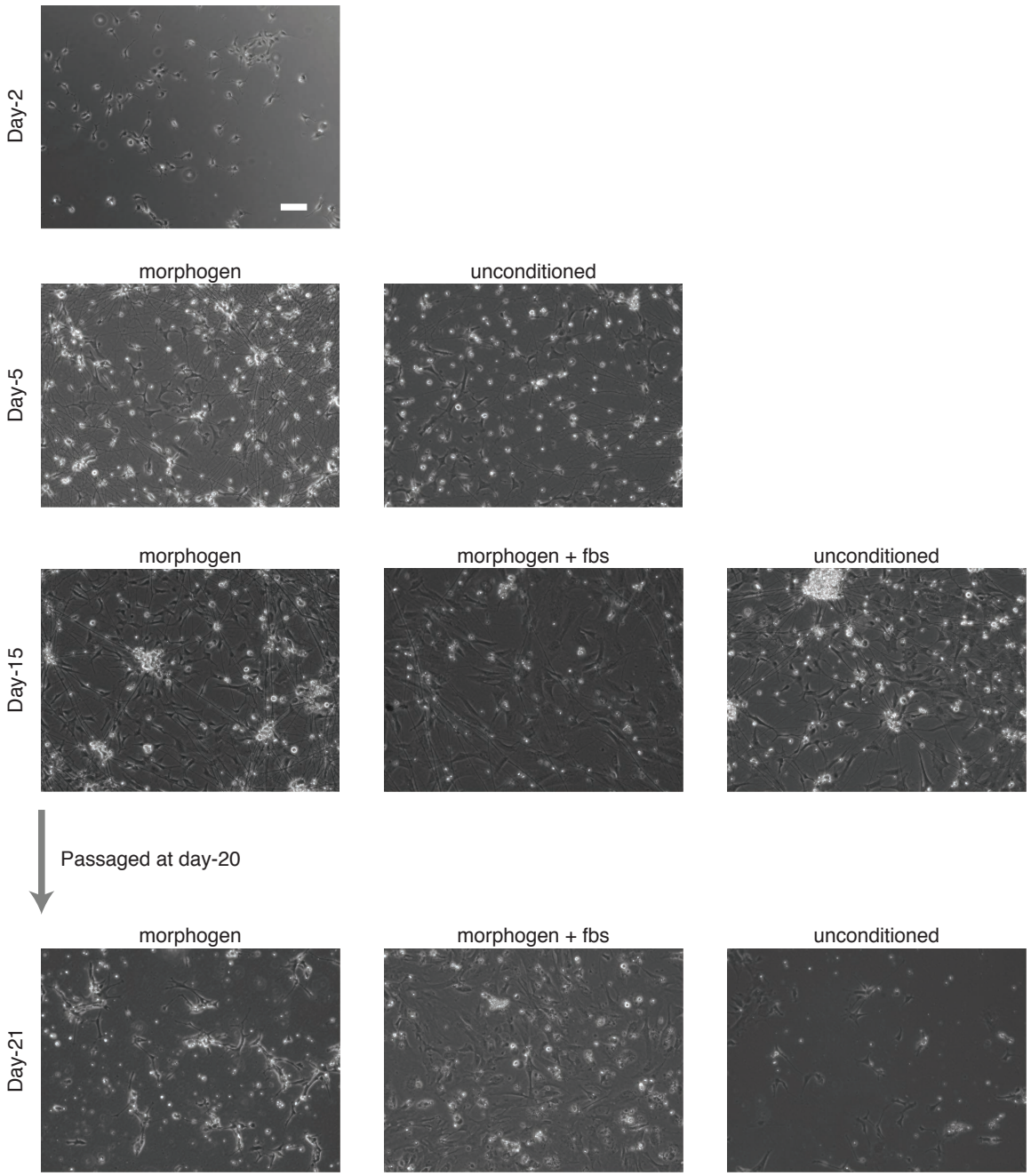

Supplementary Figure 17 | Passaging removes neuron-like cells formed during derivation of astrocytic cells from hESCs. Representative phase images of cells at day-2, day-5, day-15 and day-21 of differentiation protocols described in Fig. 6a and Supplementary Fig. 16a. Passaging cells in all conditions at day-20 removed neuron-like cells formed along with astrocytic cells during derivation protocols. Scale bar, 100 μm.

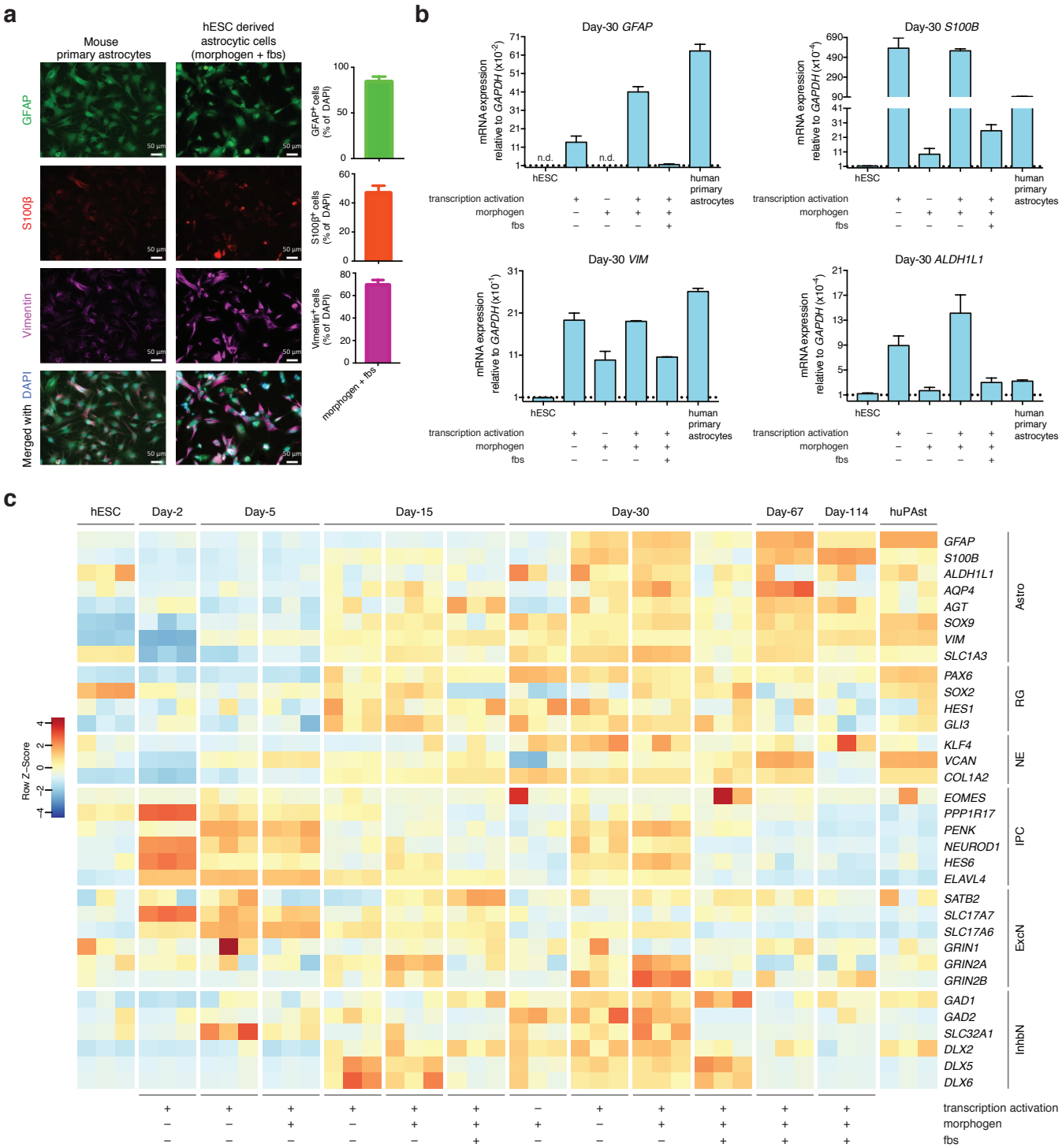

Supplementary Figure 18 | Characterization of human astrocytic cells derived from hESCs. (a) Immunostaining images of mouse astrocytes and hESC-derived astrocytic cells at day 35 for GFAP, S100β and Vimentin along with DAPI for nuclei staining. Plots show percent of GFAP$^+$, S100β$^+$ and Vimentin$^+$ hESC-derived cells at day 35 (n=3). Scale bars are 50 μm.(b) Expression of *GFAP*, *S100B*, *VIM* and *ALDH1L1* in cells in different conditions of differentiation protocols (involved transcription factors (*NGN1* and *NGN2*) used for neural induction, a morphogen (cntf, ciliary neurotrophic factor) and fetal bovine serum (fbs)) was measured at day 30. Undifferentiated hESCs were used as a negative control and human primary astrocytes were used as positive control (n=3 for all conditions and bars show mean ± SEM, and n.d. represents not-detected). (c) Expression levels of marker genes for a variety of cell types across different conditions of differentiation protocols at different time points. Undifferentiated hESCs were used as a negative control and human primary astrocytes (huPAst) were used as positive control. Astro: Astrocyte marker genes; RG: Radial Glia marker genes; NE: Neuroepithelial cells marker genes; IPC: Intermediate Progenitor Cells marker genes; ExcN: Excitatory Neurons marker genes; InhbN: Inhibitory Neurons marker genes. Color schemes are based on z-score distribution. (n=3 for all conditions).

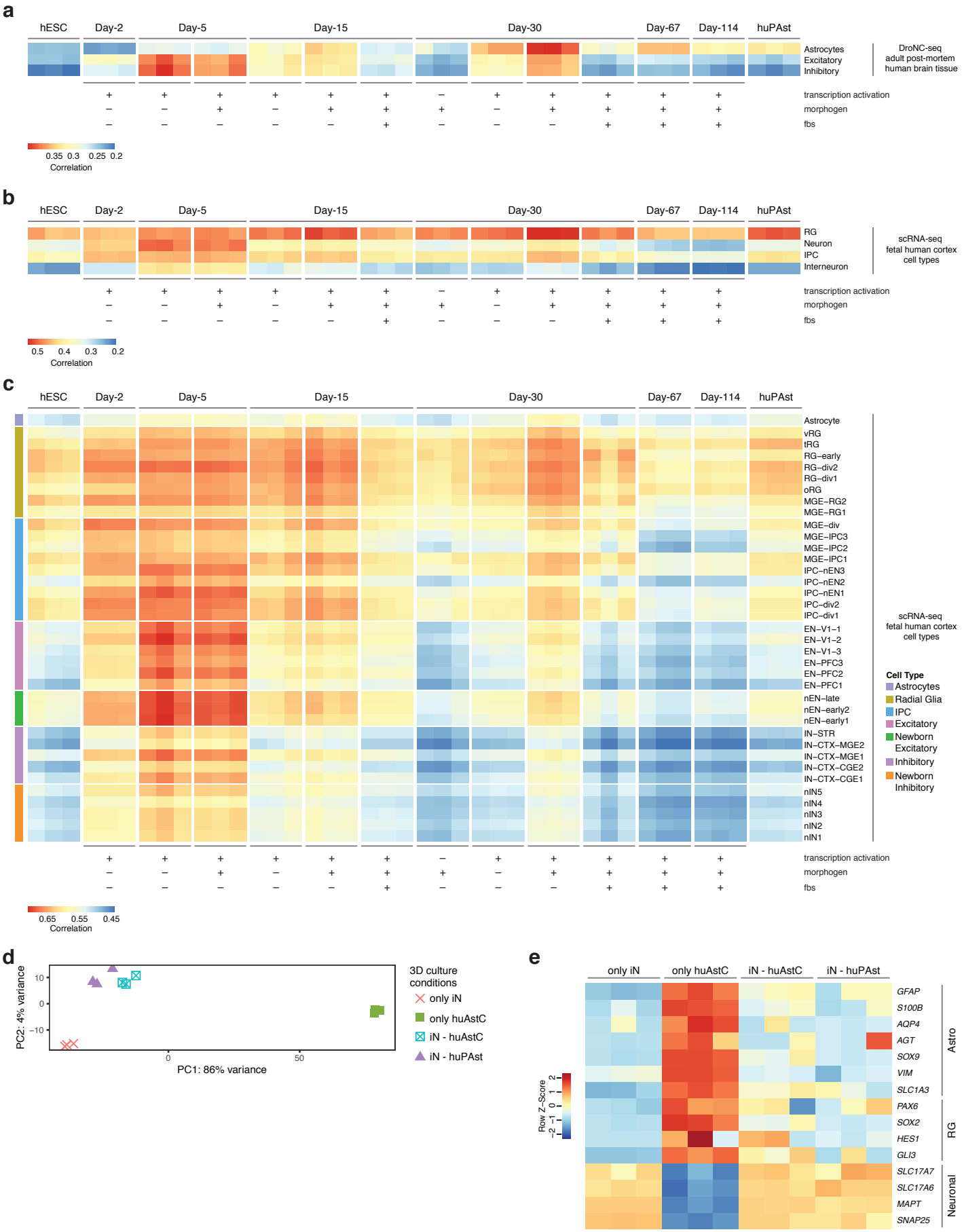

Supplementary Figure 19 | Transcriptomic correlation of cells in astrocytic cell differentiation protocols to cell types in human brain and characterization of co-culture of human iN cells with human astrocytic cells. Pearson's correlations between bulk RNA-seq data of cells in astroctytic cell differentiation protocols (involved transcription

factors (*NGN1* and *NGN2*) used for neural induction, a morphogen (cntf, ciliary neurotrophic factor) and fetal bovine serum (fbs)) at different time points as well as undifferentiated hESCs and human primary astrocytes (huPAst) were used as controls (n=3 for all conditions) (columns) and (a) cell types (Excitatory Neurons, Inhibitory Neurons, and Astrocytes) defined by DroNC-seq (single-nucleus RNA sequencing with droplet technology) in the adult post-mortem human brain tissue[8] (rows) and (b) cell types (Int-Neu: Interneurons; IPC: Intermediate Progenitor Cells; RG: Radial Glia cells) defined by single-cell RNA sequencing (scRNA-seq) in the human fetal cortex[9] (rows) and (c) cell types defined by scRNA-seq in the human fetal cortex[10] (rows). EN: Excitatory Neuron; PFC: Prefrontal Cortex; V1: Primary Visual Cortex; IN: Inhibitory Neuron; CGE: Caudal Ganglionic Eminence; MGE: Medial Ganglionic Eminence; IPC: Intermediate Progenitor Cells; RG: Radial Glia cells. See also Supplementary Table 15 for descriptions of cell type clusters defined by scRNA-seq in the human fetal cortex[10]. (d) PCA based on whole-transcriptome data of human astrocytic cells (only huAstC) cultured in Matrigel (7.36 mg/ml) and iN cells cultured (only iN) or co-cultured with either human primary astrocytes (iN - huPAst) or human astrocytic cells (iN - huAstC) in Matrigel (7.36 mg/ml) at 5 weeks. (n=3 for each condition, 10^3 iN cells were sorted from each replicate of each culture/coculture condition). (e) Expression levels of neuronal, radial glia (RG) and astrocyte (Astro) marker genes in conditions shown in (d), demonstrating minimal contamination from human astrocytic cells and human primary astrocytes among population of iN cells sorted from their co-cultures (iN – huAstC and iN – huPAst).

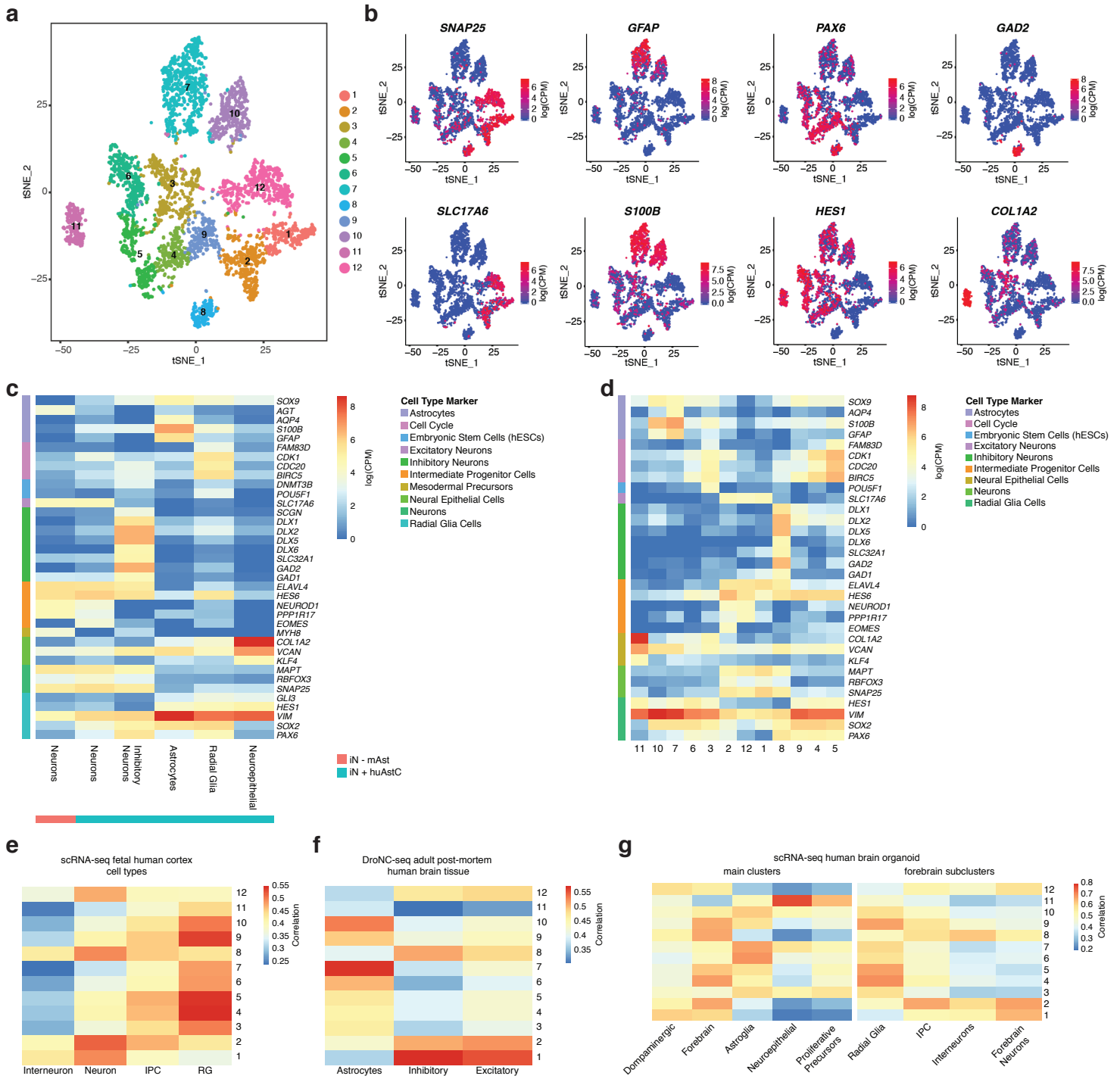

Supplementary Figure 20 | Analysis of scRNA-seq data. (a) A t-distributed stochastic embedding (tSNE) plot showing identified clusters by using Louvain clustering for scRNA-seq profiles shown in Fig. 7a, with cells colored by cluster membership. (b) tSNE plots showing expression levels of cell type marker genes for identified clusters of cell types shown in Fig. 7b with cells colored by the expression level of marker genes. CPM: Counts per million. (*SNAP25* and *SLC17A6*, neuron markers; *GFAP* and *S100B*, astrocyte markers; *PAX6* and *HES1*, radial glia markers; *GAD2*, inhibitory neuron marker; *COL1A2*, neuroepithelial cell marker). (c) Heatmap showing average expression of various cell type markers genes (rows) in identified clusters of cell types shown in Fig. 7b (columns). (d) Heatmap showing average expression of various cell type markers genes (rows) in identified clusters shown in (a) (columns). (e) Pearson's correlations between the average gene expression in identified clusters shown in (a) (rows) and cell types defined by scRNA-seq in the human fetal cortex[9] (columns). Int-Neu: Interneurons; IPC: Intermediate Progenitor Cells; RG: Radial Glia cells. (f) Pearson's correlations between the average gene expression in identified clusters shown in (a) (rows) and cell types (Excitatory Neurons, Inhibitory Neurons, and Astrocytes) defined by DroNC-seq in the adult post-mortem human brain tissue[8] (columns). (g) Pearson's correlations between the average gene expression in identified clusters shown in (a) (rows) and main clusters and forebrain subclusters defined by scRNA-seq in six-moth-old human brain organoids[11] (columns). Forebrain subclusters were derived from forebrain cluster shown in main clusters. IPC: Intermediate Progenitor Cells.

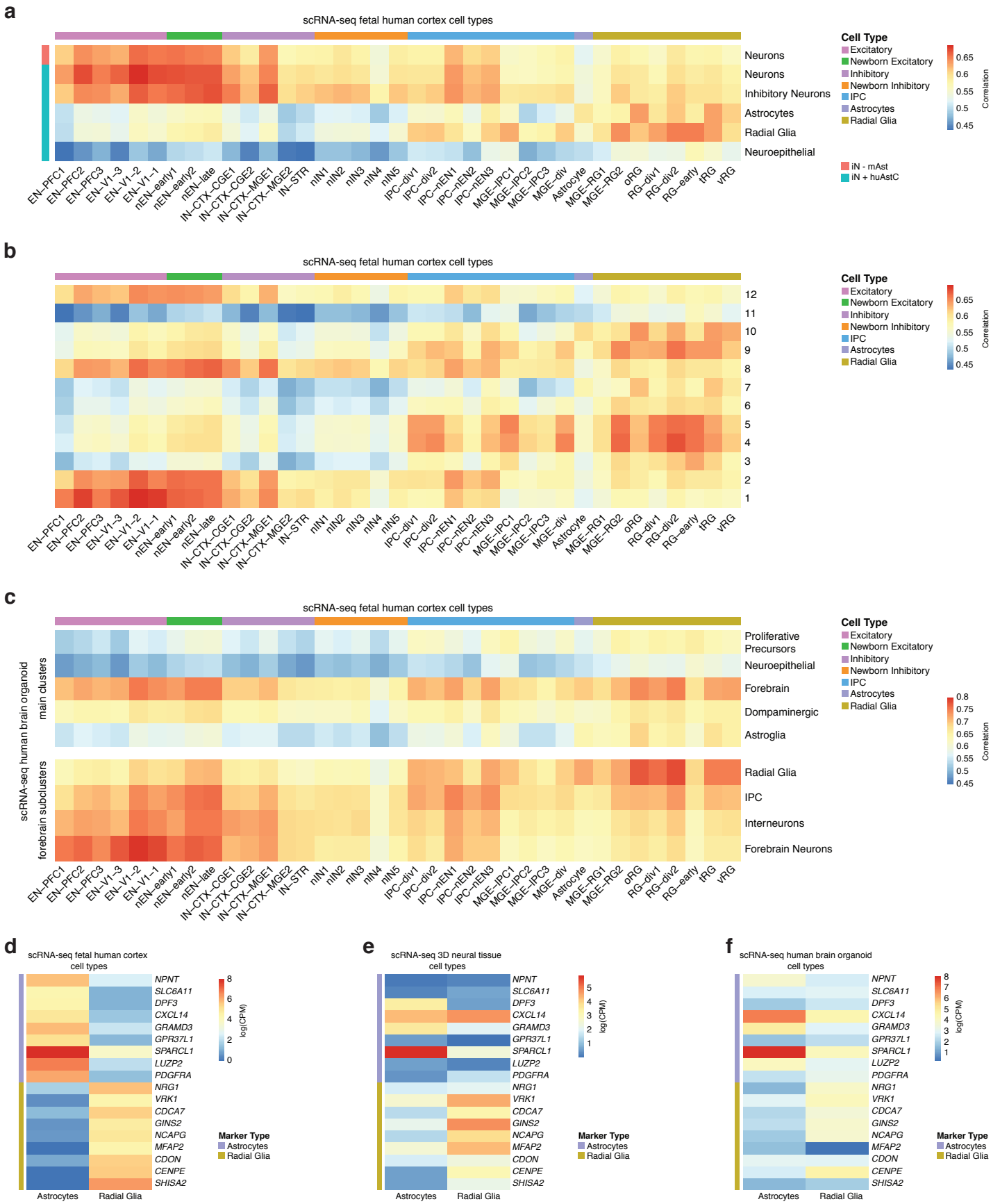

Supplementary Figure 21 | Comparison of scRNA-seq data of 3D neural tissues and scRNA-seq data of six-month-old human brain organoids to scRNA-seq data of fetal human cortex. (a) Pearson's correlations between the average gene expression in identified clusters shown in Fig. 7b (rows) and cell types defined by scRNA-seq in the human fetal cortex[10] (columns). EN: Excitatory Neuron; PFC: Prefrontal Cortex; V1: Primary Visual Cortex; IN: Inhibitory Neuron; CGE: Caudal Ganglionic Eminence; MGE: Medial Ganglionic Eminence; IPC: Intermediate Progenitor Cells; RG: Radial Glia cells. See also Supplementary Table 15 for descriptions of cell type clusters defined by scRNA-seq in the human fetal cortex[10].

(b) Pearson's correlations between the average gene expression in identified clusters shown in Supplementary Fig. 20a (rows) and cell types defined by scRNA-seq in the human fetal cortex[10] (columns). (c) Pearson's correlations between main clusters and forebrain subclusters defined by scRNA-seq in six-moth-old human brain organoids[11] (rows) and cell types defined by scRNA-seq in the human fetal cortex[10] (columns). Forebrain subclusters were derived from forebrain cluster shown in main clusters. IPC: Intermediate Progenitor Cells. (d) Differential expression analysis between astrocytes and RG cells in the scRNA-seq dataset of the human fetal cortex[10] was performed. The top 9 astrocyte-specific genes and top 9 RG-specific genes were identified based on log fold change. Heatmap showing average expression of top 9 astrocyte-specific genes and top 9 RG-specific genes (rows) in astrocyte and RG clusters defined by scRNA-seq in the human fetal cortex[10] (columns). CPM: Counts per million. (e) Heatmap showing average expression of top 9 astrocyte-specific genes and top 9 RG-specific genes (rows) in astrocyte and RG clusters shown in Fig. 7b (columns). (f) Heatmap showing average expression of top 9 astrocyte-specific genes and top 9 RG-specific genes (rows) in astrocyte and RG clusters defined by scRNA-seq in six-moth-old human brain organoids[11] (columns).

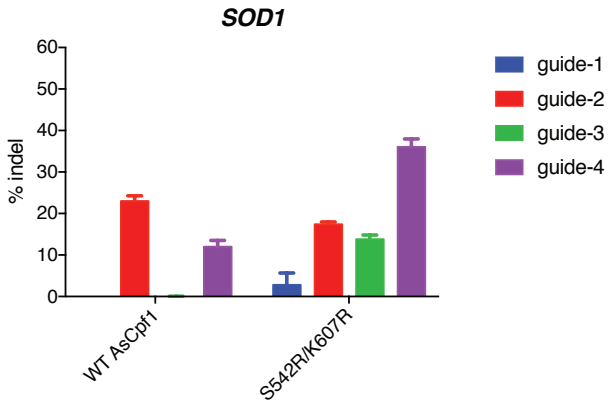

SOD1

	PAM	Target Sequence
guide-1	GCCC	TTCAGCACGCACACGGCCTTCGT
guide-2	TTTC	TGGATAGAGGATTAAAGTGAGGA
guide-3	ACCG	TGTTTTCTGGATAGAGGATTAAA
guide-4	TTCA	ATAGACACATCGGCCACACCATC

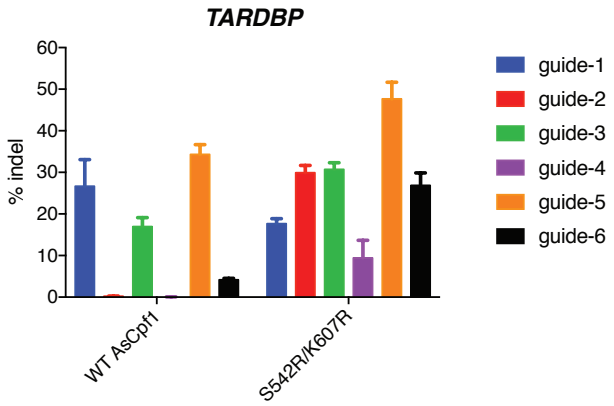

TARDBP

	PAM	Target Sequence
guide-1	TTTC	TCTTTAGGAAAAGTAAAAGATGT
guide-2	ACCC	GAATATATTCAGACATCTTTTAC
guide-3	TTCG	GTTACCCGAATATATTCAGACAT
guide-4	TCCA	GAAAACATCCGATTTAATAGTGT
guide-5	TTCC	ATGGGAGACCCAACACTATTAAA
guide-6	TTCG	GTTGTTTTCCATGGGAGACCCAA

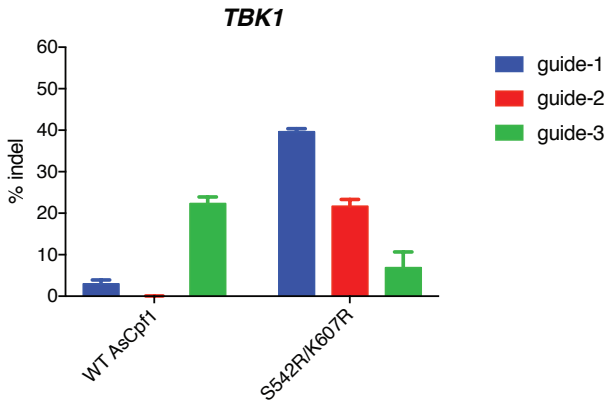

TBK1

	PAM	Target Sequence
guide-1	TCCA	GCCAAGATGCAGAGCACTTCTAA
guide-2	GCCA	CAGATGATTAGAAGTGCTCTGCA
guide-3	TTTA	ATAACATAAGCTTCCTTCGTCCA

Supplementary Figure 22 | Editing efficiencies of gRNAs for three targeted genes. Four gRNAs targeting *SOD1* locus, six gRNAs targeting *TARDBP* locus, and three gRNAs targeting *TBK1* locus were tested for efficacy with AsCpf1 (S542R/K607R) and wild-type AsCpf1 (WT AsCpf1) by transfecting HEK293FT cells. PAM and target sequences for each gRNA are shown. Plots show indel (MLE) percentages of all tested gRNAs for each targeted gene. (n=3 for each condition and bars show mean ± SEM).

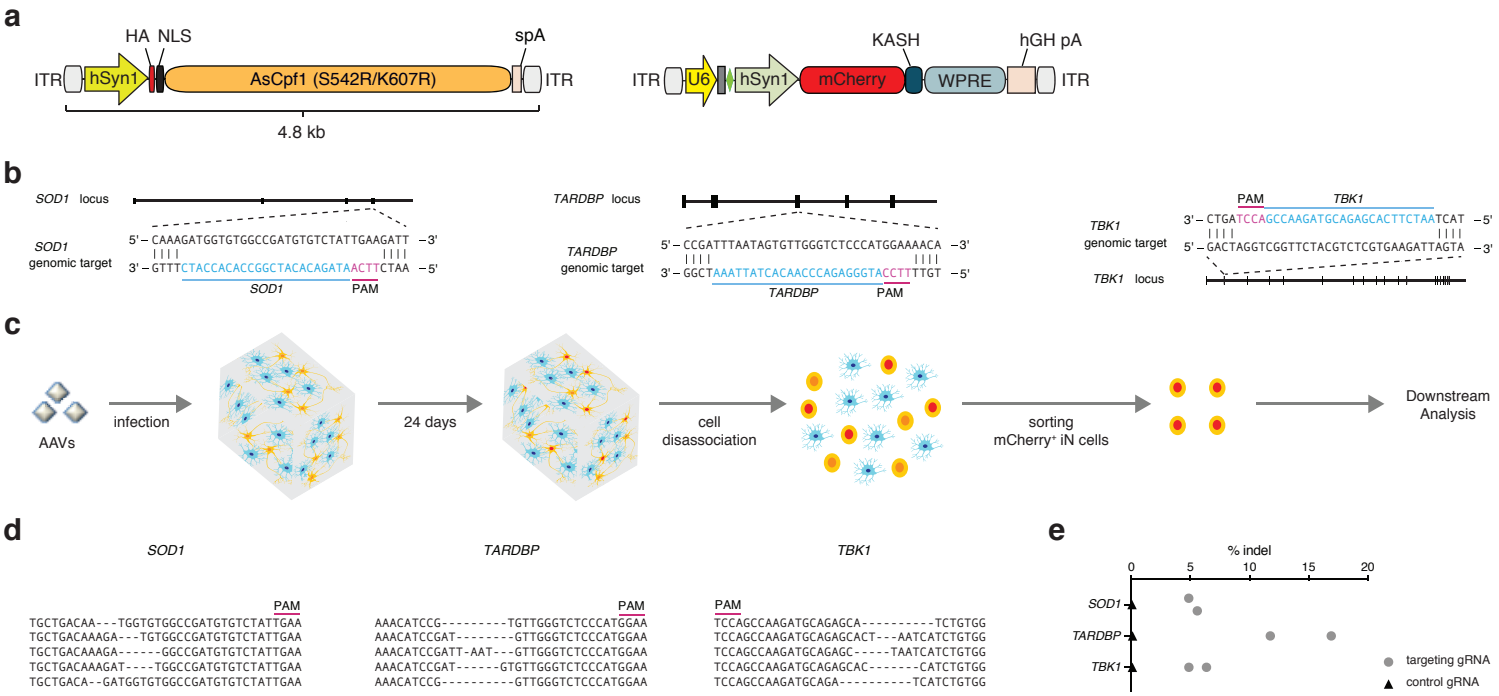

Supplementary Figure 23 | Perturbation of disease-implicated genes in 3D tissues composed of human iN and astrocytic cells. (a) Schematic of AAV vector design for gene editing using AsCpf1(S542R/K607R). Bottom: gray rectangle, direct repeat; green diamond, spacer for targeted gene. Bottom vector encodes the mCherry-KASH fusion protein for identification of transduced iN cells. (b) Graphical representation of the human *SOD1*, *TARDBP*, and *TBK1* loci displaying AsCpf1(S542R/K607R) target locations; targeted genomic locus for genes indicated in blue and PAM sequences marked in magenta (see also Supplementary Fig. 22). (c) Schematic for genome editing in 3D neural tissues. (d) Representative mutation patterns detected by sequencing of *SOD1*, *TARDBP*, and *TBK1* loci. (e) Indel analysis of Cpf1-mediated editing of *SOD1*, *TARDBP*, and *TBK1* using AAV vectors in mCherry$^+$ iN cells sorted from 3D human neural tissues (n = 2 human neural tissues for targeting guides). A total of 10^3 mCherry$^+$ iN cells were sorted for each condition.

Supplementary Tables

Supplementary Table 1 | Differentially expressed genes at 1 week between iN cells cultured in 4.6 mg/ml Matrigel and iN cells cultured on 2D.

Supplementary Table 2 | Differentially expressed genes at 5 week between iN cells cultured in 4.6 mg/ml Matrigel and iN cells cultured on 2D.

Supplementary Table 3 | Differentially expressed genes at 5 week between iN cells co-cultured with mouse astrocytes in 4.6 mg/ml Matrigel and iN cells co-cultured with mouse astrocytes on 2D.

Supplementary Table 4 | Genes in each cluster for heatmap in Fig. 2c.

Supplementary Table 5 | Genes in each cluster for heatmap in Fig. 3c.

Supplementary Table 6 I Genes ranked based on their squared log fold change in iN cells co-cultured (at total cell concentration $20x10^6$ cells/ml) in Matrigel (4.6 mg/ml) compared to the V1C brain region at 19 pcw, normalized by the squared log fold change of iN cells co-cultured (at total cell concentration $20x10^6$ cells/ml) in CH 4X CRS compared to the V1C brain region at 19 pcw, as well as Gene Ontology results for genes with score > 3 and for genes with score < -3.

Supplementary Table 7 | Genes ranked based on their squared log fold change in iN cells co-cultured (at total cell concentration $20x10^6$ cells/ml) in Matrigel (4.6 mg/ml) compared to the V1C brain region at 37 pcw, normalized by the squared log fold change of iN cells co-cultured (at total cell concentration $20x10^6$ cells/ml) in CH 4X CRS compared to the V1C brain region at 37 pcw, as well as Gene Ontology results for genes with score > 3 and for genes with score < -3.

Supplementary Table 8 | Genes ranked based on their squared log fold change in iN cells co-cultured (at total cell concentration $20x10^6$ cells/ml) in Matrigel (4.6 mg/ml) compared to the DFC brain region at 19 pcw, normalized by the squared log fold change of iN cells co-cultured (at total cell concentration $20x10^6$ cells/ml) in CH 4X CRS compared to the DFC brain region at 19 pcw, as well as Gene Ontology results for genes with score > 3 and for genes with score < -3.

Supplementary Table 9 | Genes ranked based on their squared log fold change in iN cells co-cultured (at total cell concentration $20x10^6$ cells/ml) in Matrigel (4.6 mg/ml) compared to the DFC brain region at 37 pcw, normalized by the squared log fold change of iN cells co-cultured (at total cell concentration $20x10^6$ cells/ml)

in CH 4X CRS compared to the DFC brain region at 37 pcw, as well as Gene Ontology results for genes with score > 3 and for genes with score < -3.

Supplementary Table 10 | Genes ranked based on their squared log fold change in iN cells co-cultured (at total cell concentration $20x10^6$ cells/ml) in Matrigel (4.6 mg/ml) compared to the A1C brain region at 19 pcw, normalized by the squared log fold change of iN cells co-cultured (at total cell concentration $20x10^6$ cells/ml) in CH 4X CRS compared to the A1C brain region at 19 pcw, as well as Gene Ontology results for genes with score > 3 and for genes with score < -3.

Supplementary Table 11 | Genes ranked based on their squared log fold change in iN cells co-cultured (at total cell concentration $20x10^6$ cells/ml) in Matrigel (4.6 mg/ml) compared to the A1C brain region at 37 pcw, normalized by the squared log fold change of iN cells co-cultured (at total cell concentration $20x10^6$ cells/ml) in CH 4X CRS compared to the A1C brain region at 37 pcw, as well as Gene Ontology results for genes with score > 3 and for genes with score < -3.

Supplementary Table 12 | Genes ranked based on their squared log fold change in iN cells co-cultured (at total cell concentration $20x10^6$ cells/ml) in Matrigel (4.6 mg/ml) compared to the M1C brain region at 19 pcw, normalized by the squared log fold change of iN cells co-cultured (at total cell concentration $20x10^6$ cells/ml) in CH 4X CRS compared to the M1C brain region at 19 pcw, as well as Gene Ontology results for genes with score > 3 and for genes with score < -3.

Supplementary Table 13 | Genes ranked based on their squared log fold change in iN cells co-cultured (at total cell concentration $20x10^6$ cells/ml) in Matrigel (4.6 mg/ml) compared to the M1C brain region at 37 pcw, normalized by the squared log fold change of iN cells co-cultured (at total cell concentration $20x10^6$ cells/ml) in CH 4X CRS compared to the M1C brain region at 37 pcw, as well as Gene Ontology results for genes with score > 3 and for genes with score < -3.

Supplementary Table 14 | Genes in each cluster for heatmap in Supplementary Fig. 13.

Supplementary Table 15 | Description of abbreviations for cell type clusters defined by scRNA-seq in the human fetal cortex (Nowakowski et al., 2017).

Supplementary Table 16 | Taqman qPCR probes used to measure relative RNA expression levels of a number of genes.

Gene Name	Probe ID
CXCR4	Hs00607978_s1

EPHA3	Hs00739092_m1
SEMA3C	Hs00989373_m1
UNC5C	Hs00186620_m1
NRG1	Hs01101538_m1
NTNG1	Hs01552822_m1
GPX3	Hs01078668_m1
SST	Hs00356144_m1
DAP	Hs01079452_m1
GFAP	Hs00909233_m1
S100B	Hs00902901_m1
VIM	Hs00958111_m1
ALDH1L1	Hs00201836_m1

Supplementary Videos

Supplementary Video 1 | Z-section sequences of a 3D neural tissue of iN cells cultured in 4.6 mg/ml Matrigel for 40 days stained for MAP2 (green, MAP2)(using 10X Objective).

Supplementary Video 2 | Z-section sequences of a 3D neural tissue of iN cells cultured in 4.6 mg/ml Matrigel for 40 days stained for MAP2 (green, MAP2)(using 20X Objective).

Supplementary Video 3 | Z-section sequences of a 3D neural tissue of iN cells cultured in 4.6 mg/ml Matrigel for 40 days stained for MAP2 (green, MAP2)(using 63X Objective).

Supplementary References

1 Gao, L. Y. *et al.* Engineered Cpf1 variants with altered PAM specificities. *Nature Biotechnology* **35**, 789-792, doi:10.1038/nbt.3900 (2017).

2 Zetsche, B. *et al.* Multiplex gene editing by CRISPR-Cpf1 using a single crRNA array. *Nature Biotechnology* **35**, 31-34, doi:10.1038/nbt.3737 (2017).

3 Choudhury, S. R. *et al.* In Vivo Selection Yields AAV-B1 Capsid for Central Nervous System and Muscle Gene Therapy. *Mol Ther* **24**, 1247-1257, doi:10.1038/mt.2016.84 (2016).

4 Choudhury, S. R. *et al.* Widespread Central Nervous System Gene Transfer and Silencing After Systemic Delivery of Novel AAV-AS Vector. *Mol Ther* **24**, 726-735, doi:10.1038/mt.2015.231 (2016).

5 Abel, O., Powell, J. F., Andersen, P. M. & Al-Chalabi, A. ALSoD: A user-friendly online bioinformatics tool for amyotrophic lateral sclerosis genetics. *Human Mutation* **33**, 1345-1351, doi:10.1002/humu.22157 (2012).

6 Lill, C. M., Abel, O., Bertram, L. & Al-Chalabi, A. Keeping up with genetic discoveries in amyotrophic lateral sclerosis: The ALSoD and ALSGene databases. *Amyotrophic Lateral Sclerosis* **12**, 238-249, doi:10.3109/17482968.2011.584629 (2011).

7 Nalls, M. A. *et al.* Large-scale meta-analysis of genome-wide association data identifies six new risk loci for Parkinson's disease. *Nature Genetics* **46**, 989-+, doi:10.1038/ng.3043 (2014).

8 Habib, N. *et al.* Massively parallel single-nucleus RNA-seq with DroNc-seq. *Nature Methods* **14**, 955-+, doi:10.1038/nmeth.4407 (2017).

9 Pollen, A. A. *et al.* Molecular Identity of Human Outer Radial Glia during Cortical Development. *Cell* **163**, 55-67, doi:10.1016/j.cell.2015.09.004 (2015).

10 Nowakowski, T. J. *et al.* Spatiotemporal gene expression trajectories reveal developmental hierarchies of the human cortex. *Science* **358**, 1318-1323, doi:10.1126/science.aap8809 (2017).

11 Quadrato, G. *et al.* Cell diversity and network dynamics in photosensitive human brain organoids. *Nature* **545**, 48-+, doi:10.1038/nature22047 (2017).